International Journal of Earth Sciences (2019) 108:1773–1792
https://doi.org/10.1007/s00531-019-01742-6

REVIEW ARTICLE

Marine carbonate factories: a global model of carbonate platform distribution

Julien Michel[1,3] · Marie Laugié[1] · Alexandre Pohl[1,2] · Cyprien Lanteaume[1,3] · Jean-Pierre Masse[1] · Yannick Donnadieu[1] · Jean Borgomano[1]

Received: 12 March 2019 / Accepted: 31 May 2019 / Published online: 19 June 2019

Abstract
Platform carbonates are a major component of the Earth system, but their spatial distribution through geological times is difficult to reconstruct, due to the incompleteness of geological records, sampling heterogeneity, and their intrinsic complexity. Beyond this complexity, carbonates are not randomly distributed in the world oceans, neither in the modern nor in the past, and thus, global trends exist. In the present review, we focus on the understanding of the spatial distribution of carbonate production at a global scale. We use a deterministic approach, which focuses on discriminating components, stratigraphic architectures, and environmental features to relate shallow-water carbonate production to oceanographic parameters. The work is based on extensive literature reviews on carbonate platforms. Ecological niche modelling coupled with deep-time general circulation models is used to calibrate a predictive tool of carbonate factory distribution. A carbonate factory function is set up that is based on sea-surface oceanographic parameters (temperature, salinity, and primary productivity). The model was tested using remote-sensing and in situ oceanographic data of Modern times, while outputs of paleoceanographic models are utilized for Lower Aptian (Cretaceous) modelling. The approach allows determining four neritic carbonate factories that are called the marine biochemical, photozoan, photo-C-, and heterozoan factories. The model finely simulates the global distribution of Lower Aptian and Modern carbonate platforms. Carbonate factories appear to thrive for specific ranges along the environmental gradient of carbonate saturation. This conceptual scheme appears to be able to provide a simple, universal model of paleoclimatic zones of shallow-water marine carbonates.

Keywords Carbonate factory · Carbonate prediction · Global distribution · Paleoceanographic model · Paleoclimatology

Introduction

Local sedimentary processes and the stratigraphic response of carbonate systems are influenced by specific paleogeographic contexts and local-to-global forcings, e.g., climate, currents, organic matter cycle, topography, eustasy, and tectonics (Tucker and Wright 1990; Markello et al. 2008; James and Jones 2015). The interplay between these diverse controlling factors of carbonate sedimentation at different temporal and spatial scales leads to a "conundrum" (Pomar and Hallock 2008). Predicting carbonate systems through space and time is, thus, challenging (Kiessling et al. 2003; Markello et al. 2008). The complexity of carbonate prediction is first related to the limitation of geological records due to both preservation and record, i.e., outcrop and subsurface, availability. This data limitation hampers straightforward analyses and interpretations of paleoecosystems and related sedimentation. Level of complexity also refers to the scale of observation. The study of local sedimentary records allows directly observing and analyzing sedimentary systems. Geological interpretations, however, have to face multiple, unconstrained parameters that affect the local sedimentary system, e.g., unrecorded sedimentary signatures of local hydrodynamics and paleotopography. By definition, global trends and models include large simplifications, but provide simple, efficient interpretative schemes (Lees 1975; Parrish 1982; Parrish and Curtis 1982; Schlager 2005). Thus, global

✉ Julien Michel
julien.michel@modis.com

[1] Aix Marseille Univ, CNRS, IRD, INRA, Coll France, CEREGE, Aix-en-Provence, France

[2] Department of Earth Sciences, University of California, Riverside, Riverside, CA, USA

[3] MODIS, Pau, 4 Rue Jules Ferry, Pau, France

trends and models such as the carbonate factory model of Schlager (2000, 2003, 2005) are useful tools for the extrapolation of sparse geological data. They enhance understanding of geological systems and bear some predictive power.

Such a global trend is that carbonates are not randomly distributed in the world oceans, neither in the Modern nor in the past (Lees 1975; Kiessling et al. 2003; Schlager 2005; Markello et al. 2008; Michel et al. 2018). In the Modern, the worldwide distribution of marine carbonates relates to global oceanic circulation (Lees 1975; Nelson 1988; Kleypas et al. 1999; Schlager 2005). Beyond geodynamic, biotic, and climatic evolution, the fundamental physico-chemical principles that govern both carbonate precipitation and oceanic circulation are expected to be valid throughout geological times (cf. Ridgwell and Zeebe 2005; Michel et al. 2018; Riding et al. 2019). Thus, understanding the influence of the global controlling parameters such as oceanography and climate appears critical to establish a simple conceptual model that relates carbonate production and environmental factors. The definition of such relationship would shed light on the distribution of ancient carbonate platforms (Opdyke and Wilkinson 1993; Pohl et al. 2019). In this review, we focus on the understanding of the spatial distribution of carbonate production that is controlled by sea-surface oceanographic parameters. This choice is motivated by the fact that such relationship between oceanography and carbonates provides a robust basis for the prediction of the shallow-water carbonate distributions (Lees 1975; Opdyke and Wilkinson 1990, 1993; Kleypas et al. 1999; Schlager 2005; Couce et al. 2012; Jiang et al. 2015; Pohl et al. 2019).

Sea-surface temperature was the first state variable of marine environments that was shown to control the global distribution of different carbonate grain associations (Lees and Buller 1972; Wilson 1975; Nelson 1988; Rao 1996; James 1997). Then, other environmental parameters of the marine realm such as salinity and marine productivity were shown to influence the global distribution of carbonates (Lees 1975; Henrich et al. 1995; Whalen 1995; James 1997; Wilson 2008; Westphal et al. 2010a, b). Other environmental parameters such as Ca:Mg ratio, pCO_2, and pO_2 display long-term influences on carbonate evolution, but were not shown to play any major role in the global distributional pattern of carbonate deposits at any given period of time (Stanley and Hardie 1998; Pomar and Hallock 2008; Riding et al. 2019).

Dealing with environmental controls of local case studies and evolution through time of carbonate sediments, complex models were developed to understand the occurrence and type of carbonate deposits (Tucker and Wright 1990; Markello et al. 2008; Pomar and Hallock 2008; James and Jones 2015). In contrast, no simple conceptual model is available that provides a comprehensive picture of the spatial pattern of carbonates against an integrated environmental parameter trend at a global scale; with the exceptions of distributional studies of geological records (Opdyke and Wilkinson 1993; Kiessling et al. 2003; and Markello et al. 2008) and specific studies in the Modern about Mediterranean red algae (Martin et al. 2014) and about coral reefs (e.g., Kleypas et al. 1999; Couce et al. 2012; Jones et al. 2015). The early spatial models of Lees and Buller (1972) and Lees (1975), however, greatly started the challenging spatial modelling of different carbonate associations against marine environmental parameters that are temperature and salinity (also cf. Parrish et al. 1982; Parrish 1995; for the approach). We here attempt to pursue the global spatial modelling effort to relate carbonate occurrences and environmental parameters. We build on the seminal work of Wilson (1975) about the fundamental requisite for carbonate precipitation that includes "warm waters, clear waters, water movement". Thus, we aim at defining a conceptual framework that relates a one-dimensional environmental parameter pattern with the occurrence of specific carbonate systems that are here referred to as carbonate factories. The conceptual framework aims to allow for the prediction of the global paleodistribution of shallow-water carbonate occurrences.

A carbonate factory is a carbonate precipitation mode that is defined by an ecosystem, i.e., organisms and environment, the sediments which are produced in situ and the early modification of these sediments (cf. James and Jones 2015). At the scale of the carbonate platform, Schlager (2005) described three carbonate factories based on stratigraphic and diagenetic principles, i.e., T/tropical or "top-of-the-water-column", C/cool-water, and M/microbial factories. We use a deterministic approach, which focuses on discriminating components, stratigraphic architectures, and environmental features to relate shallow-water carbonate production to ambient oceanographic conditions. This approach allows determining different carbonate factories and classifying sedimentary case studies. The primary element of control of the different factories is the source of energy driving the ecosystems and processes of mineralization such as light or nutrient concentrations (also cf. Pomar and Hallock 2008; Hallock 2015; Michel et al. 2018). In turn, the source of energy directly relates to steering oceanographic parameters that can be measured, estimated in the past and mapped, e.g., sea-surface temperature and carbonate saturation. Based on these concepts and using known oceanographic parameters, four shallow-water carbonate factories are defined, whose scheme is designed to be applied in the geological record. Another two factories are mentioned but not studied in the following.

Approach

Based on the literature and existing models, a conceptual model is developed at a global scale that relates platform-scale carbonate production and environmental parameters.

The main focus is the ecological requirements of carbonate systems to develop (e.g.. Wilson 1975). The approach of Lees and Buller (1972), Lees (1975), Opdyke and Wilkinson (1990, 1993), and Kleypas et al. (1999) is followed for the global approach relating carbonate associations and environmental parameters. A comparable approach was used to study paleogeographic distributions of source rocks, evaporites, and coals throughout the Phanerozoic (also cf. Parrish et al. 1982; Parrish 1995). The conceptual model is built upon scientific advances made by James (1997) for the distinction of phototrophic versus heterotrophic biota in carbonate grain associations, i.e., photozoan versus heterozoan association, respectively, Kiessling et al. (1999, 2003) for the global distribution approach, Schlager (2005) for the review of oceanographic controls on carbonates and the concept of platform-scale factories that is first used for a sequence stratigraphic purpose in the original work, and Pomar and Hallock (2008), Wilson (2012), Hallock (2015), and Michel et al. (2018) for the study of environmental parameters influencing carbonate production. We integrate this knowledge to develop a deterministic approach and set up a global-scale framework that predicts platform-scale carbonate production and distribution based on the first-order controlling oceanographic parameters.

The study follows the carbonate factory approach of Schlager (2000, 2003, 2005): "Each factory stands for a certain combination of environmental parameters, range of sediment composition, and depositional architecture" (Schlager 2003). The concept of the T-, C-, and M-factories comes from the definition of precipitation modes that show non-exclusive but characteristic grain associations for each carbonate factory. Each precipitation mode provides a specific production profile and sedimentary profile geometry that, in turn, show a specific conceptual model of stratigraphic architecture for each carbonate factory. Focussing on oceanographic parameters, we aim to deepen the carbonate factory classification. The conceptual approach strictly follows the one of Schlager (2005) and relates precipitation modes to non-exclusive but characteristic grain associations, sedimentary profiles, and stratigraphic architectures. These geological characteristics are the basis to classify geological case studies. The conceptual classification is then tested and validated using numerical paleoceanographic models.

Methods

This work results from extensive, including unpublished literature reviews on Phanerozoic carbonate platforms (cf. Michel et al. 2018, for Phanerozoic heterozoan carbonates; Pohl et al. 2019, for the lower Aptian period). Special focus was given to modern and paleoceanographic parameters that control carbonate production. Characteristics such as grain associations, ecological requirements, depositional profiles, stratigraphic architectures, terrigenous input, and oceanographic and basinal contexts were used to study and classify the carbonate factories that are defined at the platform scale, i.e., a carbonate platform corresponds to a single carbonate factory that is exclusive (sensu Schlager 2000, 2003, 2005; also cf. above cited references).

The relationship between modern oceanographic parameters and carbonate platforms was analyzed globally by extracting sea-surface parameter values at 1° resolution provided by GLODAPv2 (Global Ocean Data Analysis Project version 2; Lauvset et al. 2016; Olsen et al. 2016) over the zones of carbonate platforms using ArcGIS. Modern oceanographic parameters include sea-surface temperature (SST), sea-surface salinity (SSS), nutrient, i.e., PO_4, NO_3, and silicate concentrations, aragonite saturation, total alkalinity, pH, and dissolved CO_2 and O_2. Carbonate platform occurrences were identified from multiple data sets and publications including Wells (1988a, b, c; https://www.coral.noaa.gov/resources/maps.html), Lokier et al. (2009), James and Bone (2011) and a direct observation of satellite images using Google Earth. Mapping of carbonate platforms was realized using ArcGIS taking into account the whole platform area around carbonate occurrences between 0 and 200 m water depths according to the GEBCO bathymetric grid release 2014 (https://www.gebco.net/data_and_products/gridded_bathymetry_data/). A carbonate factory is assigned to every mapped platform area. Among the platform areas, a total of 80685 data points were obtained at a 0.08° resolution. A principal component analysis (PCA) was carried out on the measured variables (see Wold et al. 1987, for a complete description of the method) using the software R (R Core Team 2013). PCA and cross plots were used to highlight characteristic relationships between oceanographic parameters and global carbonate platform, i.e., carbonate factory, distribution.

Simulated environmental parameters representative of the Lower Aptian were used to compare our carbonate factory model against the rock record. An Aptian climatic simulation was conducted at 560 ppm CO_2 using the MITgcm ocean–atmosphere general circulation numerical model. A detailed description of the modelling setup is provided by Pohl et al. (2019). We used the Aptian (120 Ma) continental reconstruction of Scotese (2014a, b) that we slightly modified after the paleogeographic reconstruction of Getech, i.e., closure of the connection between the North Atlantic and Arctic Oceans (see, for instance, supplementary Fig. S1o of Lunt et al. 2016). The comparison of the simulated ocean temperatures with the recent proxy compilation of O'Brien et al. (2017) shows that such modelling setup provides climatic fields in overall agreement with the current knowledge of the Aptian mean climatic state. Simulated fields of SST, SSS, and net primary productivity (NPP) were previously

used to successfully simulate the extent of the tropical carbonate platforms during the Aptian (Pohl et al. 2019). In this study, we use the same paleoclimate model to simulate newly defined, Lower Aptian carbonate factories. To compare the results of the present carbonate factory approach with the geological record, a database of Aptian neritic carbonates was compiled based on the PaleoReef database (https://paleo-reefs.pal.uni-erlangen.de/reefs/searchreef_public.php) with additional information extracted from specific case studies (Busson et al. 1966; Busson and Albanesi 1967; Simo et al. 1993; Gili et al. 2003).

Review of environmental controlling parameters of shallow-water carbonates

Carbonates are produced by organisms that preferentially live under defined environmental conditions and by non-skeletal grains that precipitate under specific physico-chemical conditions. Thus, carbonate production should occur in defined ranges of environmental parameters including temperature, salinity, and nutrient concentrations. Because carbonates are produced by a large community of organisms, the relationship between carbonate production and environmental parameters is not straightforward. General rules, however, are well established:

- *Water temperature* Most carbonates occur in warm waters in which carbonate saturation is high and in which the energetic costs of metabolic activities are reduced (Wilson 1975; Schlager 2005). Lethal temperature thresholds of certain organisms restrict the distribution of carbonates. The paradigm of these lethal thresholds is the zooxanthellate corals, which thrive in most cases in water temperatures warmer than 18 °C year round (Veron 1995; Kleypas et al. 1999). This simple control on carbonate production helped constraining paleoclimatic interpretations, even though limitations exist (Henrich et al. 1995; Westphal et al. 2010a; Couce et al., 2012).
- *Carbonate saturation* This parameter was shown to control carbonate precipitation and distribution (Opdyke and Wilkinson 1990, 1993; Gattuso et al. 1998; Kleypas et al. 1999; Riding and Liang 2005a, b; Jiang et al. 2015). In the modern world, the distribution of carbonate saturation parallels the SST distribution (Kleypas et al. 1999; Jiang et al. 2015).
- *Salinity* Marine salinity influences the development of many organisms that might be either stenohaline or euryhaline taxa. The distribution of carbonate associations was shown to be influenced by marine salinity in both arid and humid regions (Track 1936; Opdyke and Wilkinson 1990; Lees 1975; Wilson 2012).
- *Alkalinity* Continental carbonate studies show the major role of high alkalinities in carbonate precipitation (e.g., Arp et al. 1999, 2003). In the modern marine environment, the global distribution of alkalinities is similar to the distribution of SSS due to the major influence of freshwater input (Jiang et al. 2014; Carter et al. 2014). To our knowledge, marine alkalinities were not shown to influence the global distribution of neritic carbonates apart from river-infuenced and spring-fed local environments (Beckwith et al. 2019).
- *Nutrient concentration* Ecosystems are first structured by the food web among which nutrients control the primary productivity. Thus, nutrient concentration controls the development of the biota community (Birkeland 1987; Hallock and Schlager 1986; Wood 1993; Hallock 2001; Chazottes et al. 2008; Michel et al. 2011a). On one hand, nutrient input promotes planktonic productivity within the photic zone that inhibits light-related benthic organisms such as zooxanthellate corals. On the other hand, nutrients through the development of organic matter represent the source of energy of heterotrophic biota. An excess of nutrients and associated productivity will also influence the oxic conditions of the water column that play a major role in the selection of biota development (Diaz and Rosenberg 1995; Nilsson and Rosenberg 2000; Riding et al. 2019). Upwelling occurrences, which control nutrient distribution in the ocean, play a key role in the east–west contrast in the distribution of carbonate platforms (Whalen 1995; James et al. 1999).
- *Light* As nutrient concentration, light is a major source of energy for primary producers such as algae and photosymbiotic biota including zooxanthellate corals and large benthic foraminifers. Thus, light availability, i.e., photosynthetically active radiation, controls the structure and bathymetric distribution of biological communities (e.g., Muir et al. 2015). Light through photosynthesis is also a key player of biogenic carbonate precipitation, i.e., light-enhanced calcification (Pomar and Hallock 2008; Tambutté et al. 2011).
- *Hydrodynamics* at a global scale, macrotidal such as open-ocean reefs and carbonate shelves versus microtidal regimes such as the Mediterranean Sea and gulfs (Betzler et al. 1997; Pedley and Carannante 2006; James and Lukasik 2010; James and Jones 2015), control carbonate grain associations through oceanographic circulation and the action on the seafloor substrate. The paradigm of this control is the role of wave action in reef building. Water agitation promotes carbonate calcification locally through increased gaz exchanges at the sea-atmosphere interface, i.e., CO_2 degassing, (e.g. Wilson 1975). Hydrodynamics also influence light and oxic conditions through oceanic restriction and residence time of the waters.

- *Other factors* the marine Ca:Mg ratio and pCO_2 influence carbonate sedimentation through accumulation and evolution (Stanley and Hardie 1998; Yates and Robbins 2001; Pomar and Hallock 2008; Hallock 2015). In the current knowledge, these factors, however, do not appear to control the distributional pattern of carbonates at any given period of time.

Carbonate factory scheme

Relationships between parameters and global carbonate distribution

Sea-surface waters bathing modern carbonate platforms show specific trends in oceanographic conditions. As already explained by Jiang et al. (2015), SST and carbonate saturation are positively correlated (Figs. 1, 2; see also Opdyke and Wilkinson 1990; Kleypas et al. 1999). This co-variation is opposed to the one of nutrients, oxygen, and pH. As already shown by, e.g., Carter et al. (2014) and Jiang et al. (2014), SSS and total alkalinity co-vary (Figs. 1a, 2), while global CO_2 distribution tends to show a relatively independent trend from both carbonate saturation and total alkalinity.

Carbonate precipitates in specific marine environments, preferentially those characterized by "warmth, light and water movement" (Wilson 1975; cf. also Schlager 2005). In fact, "any process which removes CO_2 from normal water (pH = 8.4), tending to change bicarbonate to carbonate ions, encourages carbonate precipitation" (Wilson 1975; also cf. Ridgwell and Zeebe 2005; the "kettle effect" of Skelton and Gili 2012). Such processes include water warming, i.e., temperature, evaporation, i.e., salinity, organic matter cycling, i.e., nutrients and carbonate cycling, i.e., normalized potential alkalinity (cf. Carter et al. 2014). Water warming decreases CO_2 solubility and, thus, increases carbonate saturation (Jiang et al. 2015). Then, increasing temperature increases the calcite and aragonite stability, thermodynamically (Hallock 2015). Thus, if the distribution of carbonates and temperatures shows good agreements (Lees and Buller 1972; Schlager 2005), it is because temperature is the first parameter that controls carbonate saturation and precipitation at a global scale (Figs. 1, 2; Opdyke and Wilkinson 1990; Kleypas et al. 1999; Carter et al. 2014; Jiang et al. 2015). Beyond the temperature threshold of modern zooxanthellate coral development, i.e., minimum of ca. 18 °C for most species (Veron 1995), warm waters promote cementation processes (Opdyke and Wilkinson 1990; James 1997; Nelson and James 2000; Nelson et al. 2003).

Marine salinity is the other major parameter that constrains global carbonate distribution, especially within the tropics (Lees 1975; Wilson 2008). Indeed, marine salinity plays a large role in carbonate equilibrium and precipitation (Track 1936; Wilson 1975; Opdyke and Wilkinson 1990; Saraswat et al. 2015; Messabeb et al. 2016; Pace et al. 2016). The global distribution of marine salinity is related to the distribution of non-skeletal grains and carbonate reef cementation (Lees 1975 and Wasserman 2011; respectively). SSS of modern carbonate platforms co-varies with total alkalinity due to the influence of freshwater influx and evaporation (Figs. 1, 2; Carter et al. 2014; Jiang et al. 2014). Therefore, at a global scale, the distribution of high alkalinities over carbonate platforms is related to the highly saline waters of the Mediterranean Sea, Red Sea, and Persian/Arabian Gulf (also cf. Brewer and Dyrssen 1985; Anderson and Dyrssen 1994). These simple observations in relation with carbonate chemistry kinetics explain that the coupling of temperature and salinity allows for a very fine modelling of modern carbonate occurrences at a global scale without explicitly accounting for the saturation state of the water (Lees 1975). Carbonate saturation is the main oceanographic parameter controlling carbonate sediment occurrences as testified by the presence of most carbonate accumulations in tropical waters (see Kleypas et al. 1999 for the Modern; Opdyke and Wilkinson 1990, 1993; Kiessling et al. 2003; and Markello et al. 2008 for the fossil record).

At a regional and local scale and away from major terrigenous inputs, steering climatic, e.g., evaporation, oceanographic, e.g., water movement, and biotic, e.g., photosynthesis, parameters control the carbonate saturation of the waters and, thus, the possibility of massive carbonate production (Wilson 1975; Pomar and Hallock 2008; Tambutté et al. 2011). While these multiple controls on carbonate precipitation show a high complexity at a local scale, the integration of key environmental parameters at a global scale can produce a fair, simple model of the global distribution of carbonate occurrences. For instance, if nutrient concentrations show diverse influences on carbonate-producing biotic communities at a local scale, the first-order global picture shows a consistent east–west contrast in carbonate platform distribution throughout geological times (James et al. 1999; Kiessling et al. 2003). Most tropical carbonate platforms occur on the western oceanic margins or equivalently eastern continental margins, e.g., West Atlantic and Indo-Pacific region (James 1997; Schlager 2005), while limited platform carbonates are found along the eastern Pacific and Atlantic margins, e.g., NW Africa (Summerhayes et al. 1976; Nelson 1988; Whalen 1995; Kleypas 2015; Martindale et al. 2015). The latter carbonates are characterized by heterotrophic carbonate-producing biota (e.g., Michel et al. 2011b).

As a summary, Fig. 1b shows the overall combination of two large oceanographic trends related to the distribution of carbonate platforms (Fig. 1b). On one hand, carbonate platforms are distributed along a global circulation trend that is characterized by latitudinal and upwelling patterns (Fig. 1, see parameters SST, carbonate saturation versus

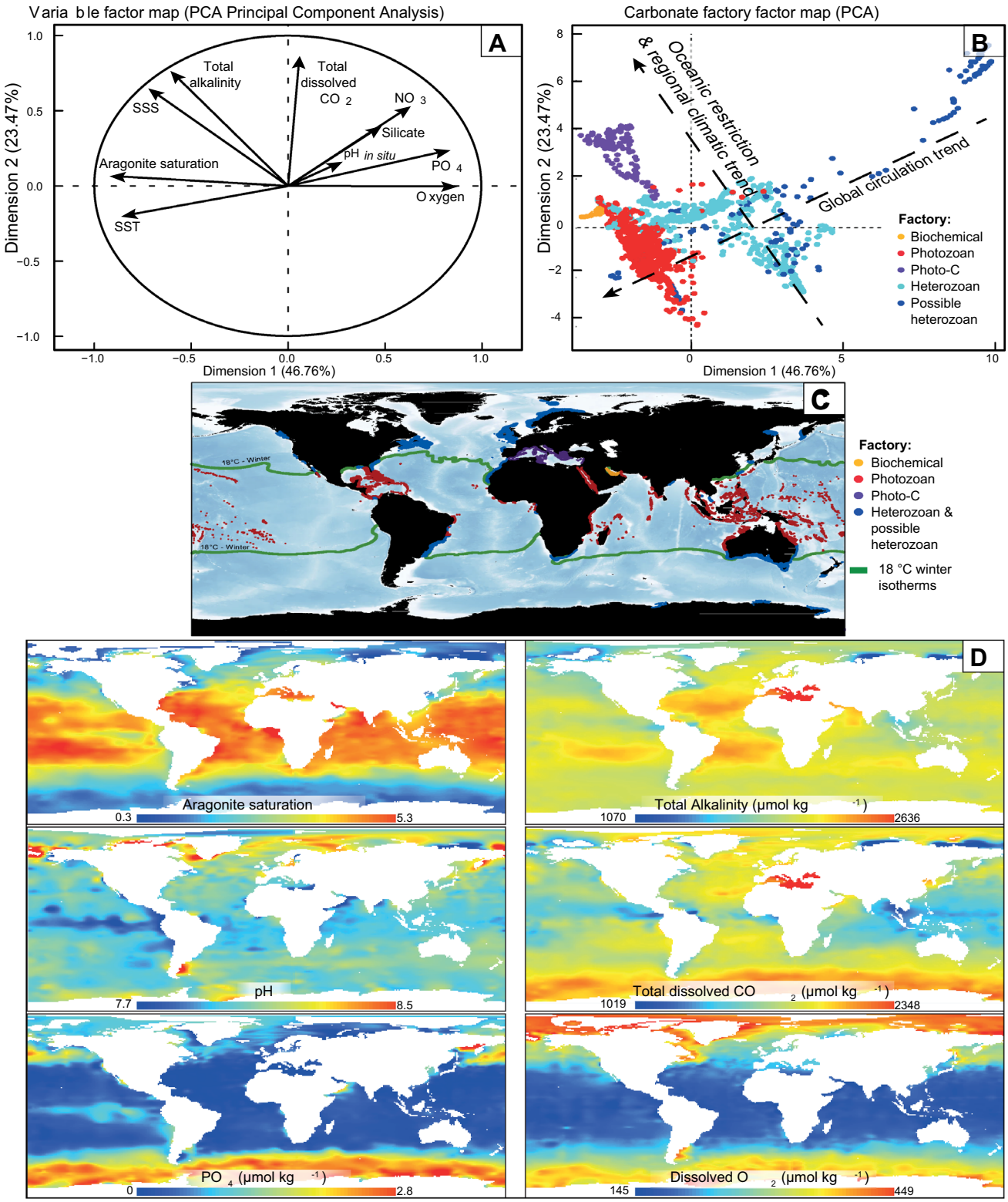

pH, oxygen and nutrients incl. phosphate, nitrate, and silicate). On the other hand, carbonate platforms are distributed along a more regional oceanographic pattern that is characterized by increased SSS and total alkalinity towards marine restricted seas and arid subtropical regions, i.e., Mediterranean Sea, Persian/Arabian Gulf, and subtropical gyres including Caribbean and Brazil (Fig. 1).

◂**Fig. 1** **a** Factor map of the sea-surface oceanographic variables from the principal component analysis (PCA) conducted over the shelfal marine zones that host the modern carbonate factories. Oceanographic factors come from the GLODAPv2 dataset (Lauvset et al. 2016; Olsen et al. 2016). **b** Factor map of the modern carbonate factories from the PCA of the sea-surface oceanographic parameters over the carbonate platform areas (see text for details). The carbonate factory "possible heterozoan" corresponds to heterozoan carbonates mapped in Lokier et al. (2009) for which no further bibliographic data were found. **c** Worldwide distribution of modern carbonate factories (modified from Laugié et al. pers. com.). The areal extent of carbonate factories is exaggerated for visualization purpose. Background bathymetric map comes from GEBCO 2014 release. **d** Global distribution of parameters of the GLODAPv2 dataset (Lauvset et al. 2016; Olsen et al. 2016). Distributional trends of sea-surface temperature (SST), sea-surface salinity (SSS), and nutrients (nitrate NO_3 and silicate) that are not shown broadly correspond to the ones of aragonite saturation, total alkalinity, and phosphate (PO_4), respectively

Carbonate factory definition

Four marine and neritic carbonate factories are defined in the following: the marine biochemical factory, the photozoan T-factory, the photo-C-factory, and the heterozoan C-factory (Fig. 3; Tables 1, 2). Another marine and neritic factory that is the automicrite or M-factory is not well constrained in the modern world and is not considered in the present analysis. The fluid-related, i.e., continental and seep, factory is excluded from the present analysis, because it is not related to global oceanographic parameters. Modern cold-water corals are also excluded from the present analysis, because major deposits are found in deep waters outside the neritic zone (e.g., Freiwald et al. 2004). In terms of oceanographic processes, cold-water corals are suspension feeders and relate to the heterozoan factory (Fig. 3).

In the Modern, the marine environment of carbonate platforms appears to discriminate the different factories (Fig. 1b). The biochemical factory occurs within the warmest waters, i.e., Persian/Arabian Gulf (Fig. 2). The photozoan, i.e., tropics, and photo-C, i.e., Mediterranean Sea, factories are well defined along gradients of temperature or carbonate saturation and salinity or alkalinity (Fig. 2). Apart from very low temperatures and very high nutrient concentrations, heterozoan factory platforms do not show any exclusive marine conditions (Figs. 1b, 2).

Definitions of factories come from the Modern but await their application in the geological past. Because carbonate factories are characterized by functional traits, i.e., ecological functions, of biota and driven by universal physico-chemical rules, they apply throughout evolutionary trends of biota and geological contexts, respectively. Types of biota and grains have changed throughout the Phanerozoic, but fundamental characteristics of factories such as oceanographic drivers, ecological systems, and sedimentary behaviors remain valid. Hence, paleogeographic, paleoclimatic, and paleoceanographic variables are expected to control the global distribution and relative contribution of carbonate factories throughout the Phanerozoic (also cf. Stanley and Hardie 1998; Pomar and Hallock 2008; Riding et al. 2019).

Carbonate factories encompass every marine carbonate platform encountered in the modern world. These carbonate factories can be characterized and discriminated by both sedimentary models and primary oceanographic parameters at a global scale. At a smaller scale, every type of carbonate factory production can occur in any platform (cf. "precipitation mode" sensu Schlager 2005). We, therefore, use a deterministic approach, which focuses on discriminating components and environmental features, to assign a single factory per platform. For instance, the Great Bahama Bank shows a rimmed isolated bank, which corresponds to a photozoan T-factory. The rimmed margin isolates flat, super-saturated shallows where whitings occur and mud and non-skeletal grains are deposited; these interior shallows are typical of the biochemical factory. At the global scale, the warm, oligotrophic, open-ocean setting combined with the presence of a significant shelf break at the platform margin assigns the Bahamas to the photozoan factory.

Photozoan factory

- *Factory* This factory corresponds to reefal platforms. General features of these platforms are described in the T-factory of Schlager (2005). The most typical characteristic of this factory is an aggrading, buildup-shaped stratigraphic architecture. Excluding the biochemical factory, the photozoan factory represents the classical *tropical carbonates* (cf. Wilson 1975, "shelf margin complexes at the edges of major basins or along margins of major offshore banks within such basins, areas of considerable subsidence") or photozoan carbonates (James 1997).
- *Depositional setting and components* The photozoan factory typically corresponds to the tropical carbonate shelf or the detached rimmed platform that are characterized by phototrophic skeletal grains and reefs and the highest rates of carbonate production ("shelf margin complexes" of Wilson 1975; Tucker and Wright 1990; James 1997). This factory comprises corals, stromatoporoids, algae in particular green algae, sponges, and photosymbiotic benthic foraminifers (cf. James 1997). Because they are restricted to shallow tropical waters and occur within carbonate platforms that show platform margins and occur in rather oligotrophic oceanic regions (Föllmi et al. 2006; see Pohl et al. 2019 for more details), rudist-rich platforms are included in the photozoan factory.
- *Depositional environment and parameters* Because light is the main source of energy controlling the development of the photozoan factory, the distribution of the factory is restricted to low-latitude, warm, and clear oce-

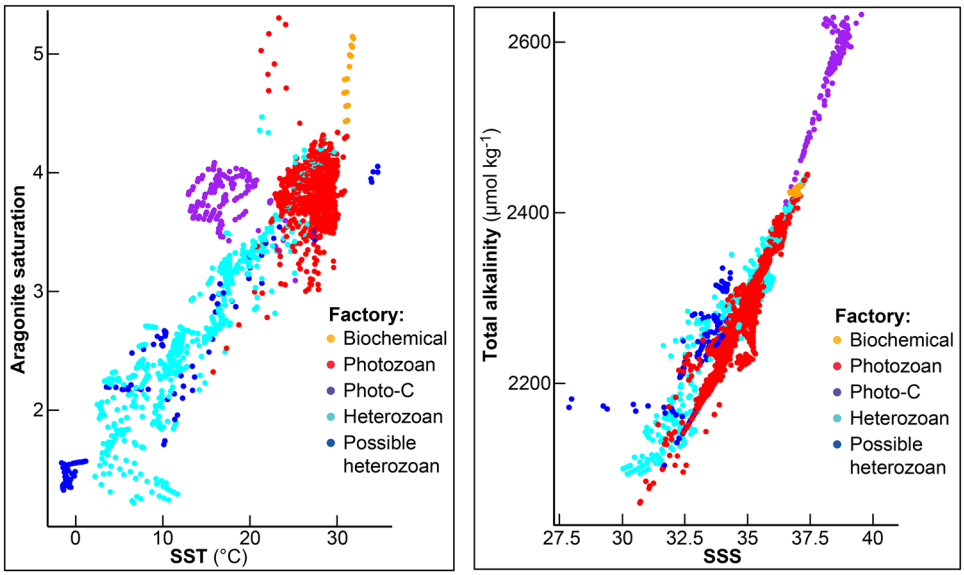

Fig. 2 Relationship between sea-surface temperature and aragonite saturation (left) and sea-surface salinity and total alkalinity (right) of the sea-surface waters over the carbonate platform areas (see text for details). The carbonate factory "possible heterozoan" corresponds to heterozoan carbonates mapped in Lokier et al. (2009) that remain bibliographically unconstrained. Oceanographic data come from the GLODAPv2 data set (Lauvset et al. 2016; Olsen et al. 2016)

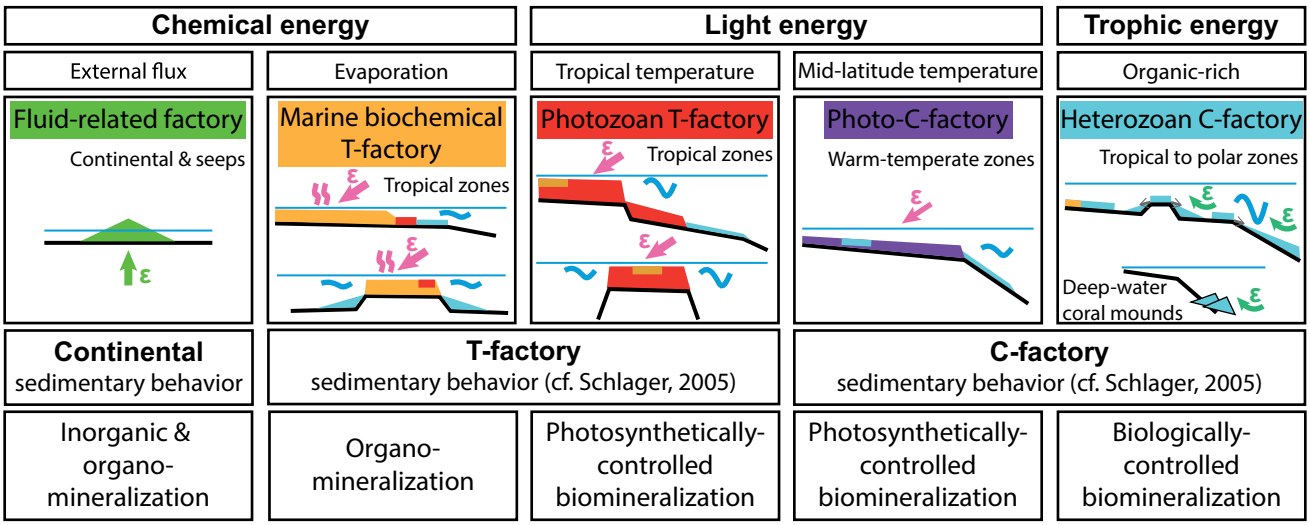

Fig. 3 General overview of the conceptual carbonate factory scheme that relates carbonate deposits and oceanographic parameters at a global scale. Heterozoan carbonates sensu James (1997) are split into two carbonate factories (i.e., heterozoan and photo-C-factories); photozoan carbonates sensu James (1997) are split into two carbonate factories (i.e., marine biochemical and photozoan T-factories). Seep and continental carbonates (fluid-related factory) that are not included in the present study are considered separately. Mineralization terminology following Schlager (2005) and Dupraz et al. (2009)

anic waters. James and Bourque (1992) give a temperature range of occurrence of 18–36 °C with an optimum between 25 and 29 °C and a wide salinity range of 22–40 psu (practical salinity units) with an optimum between 25 and 35 psu (Fig. 2; also cf. chlorozoan grain association of Lees 1975; Kleypas et al. 1999, for coral reefs). In the Modern, the photozoan factory shows particular adaptations for oligotrophic settings, i.e. < 0.3 mg Chl-*a* m^{-3} (Hallock 2001). The coupling of photosynthesis and calcification is seen as the driving mechanism for high carbonate production rates that correspond to the photosynthetically enhanced calcification biological process (e.g., Tambutté et al. 2011) throughout geological times (see Pomar and Hallock 2008). Relatively strong hydrodynamics and well-oxygenated waters are thought to control the reef or margin building capacity or accumulation through winnowing and cementation processes (e.g., Perry and Hepburn 2008).

- *Examples of the photozoan factory* Modern platforms are found in the Caribbean, Red Sea, Indo-Pacific islands, and Great Barrier Reef. The modern distribution of this factory corresponds to the one of shallow-water coral

Table 1 Basic conceptual scheme defining key characteristics and environmental parameters of modern marine carbonate factories (cf. text for details)

Factory	Composition (characteristic)	Composition (secondary)	Textures (characteristic)	Oceanographic conditions	Marine environment	Mound and reef structures	Sedimentary signature
Marine biochemical T-factory	Evaporites, algal mats, stromatolites and other microbes, non-skeletal grains, muds	Any bioclast	Bindstone; mudstone and dolomite	Very high supersaturation (very high temperature and salinity)	Restricted, shallow waters (epicontinental platforms)	? Mud mounds (→ automicrite factory?)	Peritidal facies, homoclinal ramp
Photozoan T-factory	Phototrophic biota, corals, rudists, ? large benthic foraminifers	Any grain	Frame-bafflestone; mudstone	High supersaturation (high temperatures); oligotrophic	Shallow, eu-mesophotic open-ocean waters	Barrier reef; coral-algal-stromatoporoid mounds	Rim, large "reefs"
Photo-C-factory	Red algae, large benthic foraminifers, seagrass-derived bioclasts	Any bioclast including subordinate corals	Grain-rudstone; packwackestone	Eu-mesophotic, oligo-mesotrophic	Subtropical/warm-temperate, restricted seas	None (rhodoliths and encrusting algae, shoals)	Distally steepened ramp
Heterozoan (C-factory)	Heterotrophic biota	Any subordinate grain	Grainstone; packwackestone	Eutrophic	Upwelling-influenced open-ocean platforms	None (shell beds)	Shell beds, continental shelf
Automicrite (M-factory)	Microbes and micrites	(mega)breccias	Bindstone, micrite	? Dysoxia, very high supersaturation	? Restricted waters at a basinal scale	Mud mounds	Cohesive sediments and steep slopes

The fluid-related (continental and seep) factory that is not included in the present study is shown

Table 2 Key but non-exclusive characteristics of the marine carbonate factories (cf. text for details)

Characteristics	Fluid-related	Marine biochemical	Photozoan	Photo-C	Heterozoan
Energetic source for carbonate production	Water chemistry		Light		Organic matter (marine productivity)
	Non-marine fluids (extrinsic)	Carbonate saturation (evaporation)	Tropical light	Tropical-to-temperate light	
Oceanographic controlling parameters	Seep and pore waters	Highest temperature, high salinity	High temperature and light penetration	Mid-latitude seasonal variability (high-to-moderate temperature and light penetration)	Food supply (upwelling and runoffs)
Characteristic depositional environment	Continental and seep environments	Homoclinal ramp (restricted water bodies)	Reefal platforms	Mediterranean-type, distally steepened ramp	Open-shelf upwelling and nutrient-rich platforms
Basin type	(Local accumulations)	Epicontinental platforms and foreland basins	Open-ocean, isolated topographic highs and exposed shelves	Microtidal seas and gulfs	Open ocean
Stratigraphic architecture trend	Fluid-source-dependent	Prograding-retrograding trend	Aggrading trend (cf. T-factory of Schlager 2005)	Prograding trend (cf. C-factory of Schlager 2005)	Transport-controlled prograding trend (cf. C-factory of Schlager 2005)

The automicrite or M-factory that is not included in the present study is shown

reefs (cf. Kleypas et al. 1999). Ancient examples are associated with rimmed shelves and aggrading buildups. Typical examples include Cenozoic platforms from South-East Asia and the Indian Ocean and Cretaceous rudist-rich platforms from Europe. A possible Paleozoic example of this photozoan factory is Carboniferous platforms from Kazakhstan. Wilson (1975) also mentions Cretaceous to modern Bahamas, Cretaceous Valles, and Golden Lane platform from central Mexico, and Silurian pinnacle reefs from the Michigan Basin. Paleozoic examples might, however, include M-factory case studies (cf. Reijmer 2014).

Biochemical factory

- *Factory* This factory corresponds to the model of "shelf strata laid down across flat cratonic areas in clear epeiric seas, areas of moderate subsidence" of Wilson (1975), and includes the neritic lime-mud factory of Pomar and Hallock (2008), the peritidal factory (James and Jones 2015), and several shallow-water, microbially induced carbonate precipitations such as the production of ooids and stromatolites (Pomar and Hallock 2008; also cf. organomineralization sensu Dupraz et al. 2009; Diaz and Eberli 2019). The most typical characteristic of this factory is an up-to-100 s-of-kms-wide, layer-cake stratigraphic architecture.
- *Depositional setting and components* This factory is typically a tropical carbonate ramp characterized by a low-angle of repose, i.e., homoclinal ramp, and by non-skeletal grains as characteristic components (cf. Opdyke and Wilkinson 1990). The platform of the biochemical factory comprises extensive evaporitic (sabkha), peritidal, and shallow-water microbial deposits, e.g., stromatolites (cf. Dupraz et al. 2009), shells (especially molluscs), ooids, peloids, algal mats, and muds. Whitings are typical features of this factory that also shows extensive grainy skeletal deposits, e.g., bivalves, in more distal settings.
- *Depositional environment and parameters including platform examples* The biochemical factory occurs in a marine setting showing high temperatures and salinities (Fig. 2), a restricted oceanic circulation and relatively moderate-to-low hydrodynamics. This marine realm favors a very high carbonate saturation that is the driver of the biochemical factory (cf. the "kettle effect" process of Skelton and Gili 2012; Lowery and Rankey, 2017). The modern example of this factory is the Persian/Arabian Gulf (cf. Purser 1973; Lees 1975; Wilson 1975; Tucker and Wright 1990; Riegl et al. 2010) that displays SSS up to > 40 psu and SST up to > 30 °C (Riegl et al. 2010). While they are not considered as photozoan factories at the scale of the platform, the Shark Bay and

the top of the Great Bahama Bank represent additional examples of carbonate production and environmental conditions of the biochemical factory (cf. Opdyke and Wilkinson 1990; Lowery and Rankey 2017; Diaz and Eberli 2019).

- *Examples of the biochemical factory* Typical depositional environments through geological times include shallow, warm intracratonic basins, e.g., Paleozoic platforms from the North American craton, epicontinental platforms, e.g., Oligo-Miocene platforms from North Africa and the Cretaceous platforms from the northern Gulf of Mexico area, and foreland basins, e.g., Asmari Formation from the Zagros Basin. Wilson (1975) also mentions the Mississippian Williston Basin, the Central Montana high region, and Albian platforms from central Texas. Due to these paleogeographic characteristics and the higher oceanic carbonate saturations prior to the Mesozoic pelagic carbonate development (Ridgwell and Zeebe 2005), it is expected that the distribution of the biochemical factory was more widespread during the Paleozoic and Mesozoic periods (cf. Opdyke and Wilkinson 1990, 1993).

Photo-C-factory

- *Factory* This factory corresponds to the microtidal cool-water factory of Pedley and Carannante (2006), the protected-setting type of the warm-temperate carbonates of Betzler et al. (1997; also cf. James and Jones 2015), the Mediterranean platform scheme of Pérès and Picard (1964), the photozoan–heterozoan transition of Halfar et al. (2004), and the subtropical carbonates of Bensing et al. (2008). This factory was described as red algae/seagrass platforms of oligo-mesotrophic, warm-temperate settings in Michel et al. (2018). Compared to the previously mentioned tropical carbonate factories, the photo-C-factory shows much smaller carbonate accumulations that are characteristic of the C-factory in terms of stratigraphic architectures (cf. Schlager 2005).
- *Depositional setting and components* The photo-C-factory typically forms distally steepened ramps (Pomar 2001) and comprises proximal seagrass-derived bioclastic sediments (Perry and Beavington-Penney 2005; James et al. 2009a) and distal red algal accumulations, i.e., rhodoliths and coralligenous (Pérès and Picard 1964; Bosence and Pedley 1982; Bosence 1983). Red algal deposits can be absent from the photo-C-factory in which large benthic foraminifers characterize the sediment composition (Bensing et al. 2008). This factory shows a diverse bioclastic composition in which phototrophic large benthic foraminifers and red algae form characteristic accumulations (Pedley and Carannante 2006).
- *Depositional environment and parameters* The photo-C-factory typically occurs in the warm-temperate or subtropical province, which shows a marked seasonality, i.e., 10–25 °C, and a relatively low primary productivity, i.e., < 1 mg Chl-*a* m^{-3} (Henrich et al. 1995; Betzler et al. 1997; Hallock 2001). This distribution is found at the outer limits of warm, well-saturated, tropical seas, which commonly show limited seasonal variations (Fig. 2). Light is the steering environmental factor controlling the factory distribution. Even though the photo-C-factory shows a greater tolerance to turbidity and marine productivity than the photozoan factory (cf. Hallock and Schlager 1986), deepest occurrences, and highest rates of production develop in well-illuminated settings. The photo-C-factory appears to be best adapted to moderate hydrodynamic settings (cf. Pérès and Picard 1964; Henrich et al. 1995; Pedley and Carannante 2006; Dutertre et al. 2015).
- *Examples of the photo-C-factory* The Mediterranean Sea is the main representative marine realm of this factory (Pérès and Picard 1964; Henrich et al. 1995). Southern Australian Spencer and St Vincent gulfs also represent a typical environment of this factory (James and Bone 2011; O'Connell et al. 2016). Due to seagrass and red algae evolution (cf. Riosmena-Rodríguez et al. 2017), this factory is expected to occur mostly during the Cenozoic period. Although coral reefs occur within carbonate associations, Oligo-Miocene ramps from the northern Mediterranean region show the characteristic features of the photo-C-factory, i.e., grain associations characterized by red algae and foraminifers (cf. Michel et al. 2018), ramp depositional profiles (cf. Pomar et al. 2017), C-factory stratigraphic architectures (cf. Schlager 2005), and relatively thin rock packages, i.e., typically tens-of-meters-thick, e.g., Castelcucco (Bassi and Nebelsick 2010), Porto Badisco (Pomar et al. 2014), and Sedini (Tomas et al. 2010). Formations from Italy, Cala di Labra Formation from France (Tomassetti and Brandano 2013), Amposta Limestone (Carannante et al. 1988), and Valencia Trough (Bover-Arnal et al. 2017) from Spain and Lagos-Portimao Formation from Portugal (Brachert et al. 2003). Permian subtropical ramps from the Barents Sea that show a large benthic foraminifer-rich carbonate grain association are part of this photo-C-factory (cf. Bensing et al. 2008).

Heterozoan factory

- *Factory* This factory corresponds to the heterozoan carbonates of James (1997) excluding the photo-C-factory (also cf. Halfar et al. 2004), the C-factory of Schlager (2005), and the so-called *cool-water* carbonates, in general (e.g., Nelson 1988; Henrich et al. 1995; Rao 1996). This factory was described as heterotrophic biota platforms of eutrophic settings by Michel et al. (2018). The

heterozoan factory sedimentation is first characterized by transport processes (cf. C-factory of Schlager 2005; Michel et al. 2018).

- *Depositional setting and components* The heterozoan factory forms ramps, the deposition of which is controlled by the coupling of initial topography and hydrodynamics (Michel et al. 2018). This factory is characterized by heterotrophic biota such as bryozoan- and mollusc-accumulations. Phototrophic biota and components of the biochemical factory can be present, in particular in well-illuminated, super-saturated proximal settings (Klicpera et al. 2015; Lowery and Rankey 2017). Macroalgal kelp forests can be a structural element of the ecosystem (Henrich et al. 1995; James et al. 2013). The heterozoan factory can occur in mixed carbonate-siliciclastic environments. It is worth noting that the "characteristic grains" of this factory are found in every sedimentary system, in every carbonate factory and siliciclastics.
- *Depositional environment and parameters* Marine productivity as food is the source of energy driving the development of the heterozoan factory. Consequently, the factory occurs in nutrient-rich, organic-rich, and plankton-rich marine realms such as upwelling areas and coastal zones influenced by fluvial runoff, i.e., 1–10 mg Chl-*a* m^{-3} (Hallock 2001). The depositional environment of the heterozoan factory is characterized by high hydrodynamics (Michel et al. 2018).
- *Examples of the heterozoan factory* Modern examples are found in various highly mesotrophic to eutrophic settings including the Gulf of California (Halfar et al. 2006), Yucatan (Lowery and Rankey 2017), Panama (Reijmer et al. 2012), Mauritania (Klicpéra et al. 2015), South Australia (James and Bone 2011), New Zealand (Nelson et al. 1988), and Norway (Henrich et al. 1997; Freiwald 1998). Ancient examples are associated with paleo-upwelling regions (Whalen 1995; Martindale and Boreen 1997; Franseen 2006; James et al. 2009b; Frank et al. 2012; Martindale et al. 2015). An exhaustive list of case studies is provided by Michel et al. (2018).

Automicrite factory

The microbial factory was defined by Schlager (2000, 2003, 2005; M-factory; also cf. Reijmer 2014) and re-defined by Pomar and Hallock (2008) as the benthic automicrite factory. This factory typically produces cohesive sediments and builds carbonate platforms with very steep slopes. The automicrite factory is produced by microbial activity degrading large amounts of organic matter on the seafloor under sub-oxic conditions. This process of bacterial decay producing ammonia (cf. Wilson 1975) or sulfate reduction (cf. Schlager 2005) leads to a local increase of the carbonate saturation of the seawaters. Production can occur from the euphotic to aphotic depths. Organic matter content and oxic conditions appear to constitute major drivers of this factory. No "environmental calibration", however, is available for this factory due to the absence of such carbonate platforms in the modern world. The automicrite factory produced numerous carbonate platforms during the Early Mesozoic (Trias and Jurassic). Microbialites of the Tahitian reefs might represent a modern analog of automicrite precipitation which conditions of production, however, remain poorly constrained (e.g., Camoin et al. 2006).

Seep and continental factory

Seep carbonates are produced down to abyssal depths by microbial activity and chemosymbiotic organisms, e.g., bivalves and worms, using, for instance, methane as their source of energy (e.g., Case et al. 2015). This factory is not taken into account here, because it is not related to sea surface and global oceanographic processes.

Application of the conceptual scheme to the fossil record

The process-based conceptual scheme of carbonate factories first aims to identify global-scale processes that drive the production of specific types of carbonates, i.e., grain associations and carbonate architectures (cf. Schlager 2005). When combined with environmental constraints provided by numerical paleoclimatic simulations, the scheme further gains some predictive power. An attempt of such prediction of past carbonate occurrences and a description of the methods were proposed by Pohl et al. (2019). The latter study dealt with the prediction of the tropical carbonate platforms of the Lower Aptian. We here follow up on this study to propose the prediction of specific carbonate factories based on modelled paleoceanographic constraints.

Lower Aptian tropical platforms were shown to occur between the paleolatitudes 40°N and S and on the western margin of paleo-oceans (Fig. 4). These tropical carbonates were considered and modelled as a whole in the pioneering work of Pohl et al. (2019). In-depth, i.e., case by case, deterministic study of the geological database allows distinguishing three subgroups within these Lower Aptian tropical platforms: the photozoan, biochemical, and Orbitolinid factories; the three factories being mutually exclusive. Lower Aptian platforms of the biochemical factory are characterized by widespread supratidal, intertidal, and non-skeletal grains over very extensive attached ramps, i.e., dolomitic, tidal flat, lagoonal, and oolitic deposits (Bedout et al. 1981; Scott 1993; Wilson and Ward 1993; Lehmann et al. 1999). The platform margin also shows coral- and rudist-rich sediments (Scott 1993; Fritz et al. 2000). The photozoan factory

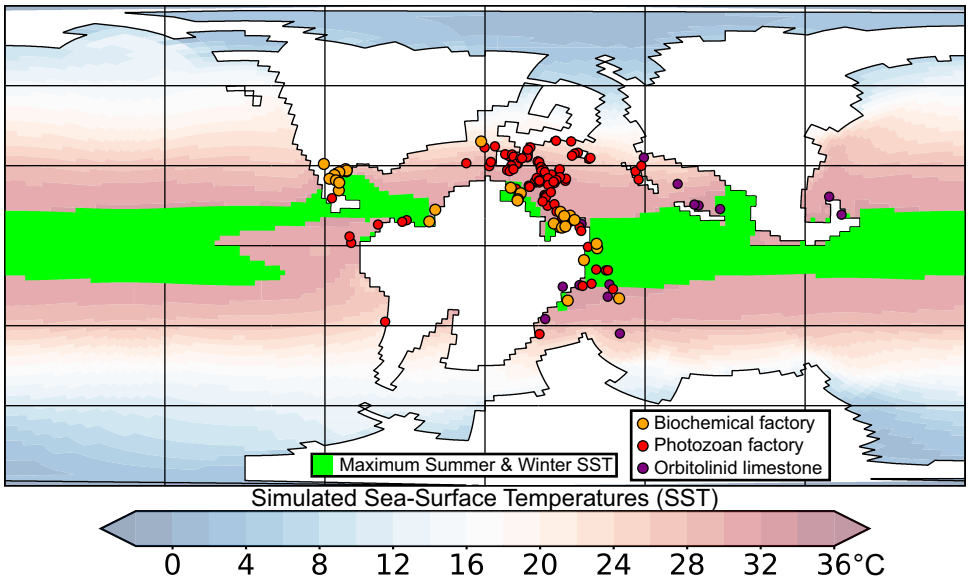

Fig. 4 Prediction of the spatial occurrences of the Lower Aptian biochemical factory based on simulated fields of sea-surface temperature (SST; 120 Ma; green shading). The green shading shows the areas of maximum simulated SST, which corresponds to boreal summer SST > 34.1 °C or austral summer SST > 31.4 °C. Carbonate factory dots (using larger dots for the biochemical factory) correspond to bibliographic reference points of marine carbonate platforms of the Lower Aptian period. Background shading is the mean annual SST simulated using MITgcm ocean–atmosphere general circulation model shown at the climate model resolution. Continental masses are shaded white. Note that most biochemical factory dots are found within the zones of maximum SST on platforms that are thought to show a high seawater surface:volume ratio

then corresponds to rudist-rich platforms that are characterized by skeletal grains. Due to limited data availability, no direct evidence of stratigraphic architecture differences was highlighted between both carbonate factories. The Orbitolinid factory corresponds to limestone beds characterized by abundant Orbitolinid shells (e.g., Ethiopia, Bosellini et al. 1999; Japan, Iba et al. 2011; Iran, Schlagintweit et al. 2013). Mollusc-rich sediment beds within siliciclastic successions are not considered here (e.g., Kazakhstan, Prosorovsky 1990; Australia, Campbell and Haig 1999).

The comparison of the Lower Aptian occurrences of the biochemical factory with the simulated field of SST suggests that the latter occurrences are restricted to the warmest oceanic regions ($n = 26/33$; Fig. 4). Occurrences of the photozoan factory generally do not overlap with the biochemical factory ($n = 13/100$ of photozoan factory distributional overlap). These photozoan factories are mostly found within relatively low paleolatitudes away from high primary productivities (cf. Pohl et al. 2019) and from the warmest temperatures (Fig. 4). The southern Asian paleoregion mostly shows opportunist-orbitolinid-rich limestone beds (Pittet et al. 2002; Föllmi et al. 2007; Embry et al. 2010), the distribution of which is thought to rely primarily on the regional input of terrigenous material in the context of the extensive volcanic arcs (Takahashi 1983) rather than on specific oceanographic settings (see discussion by Pohl et al. 2019). The climatic control on the development of the Orbitolinid-rich association may be weak, thus explaining why the latter distribution is difficult to predict at a global scale based on our paleoclimatic simulations. Since the photozoan and biochemical factories are related with key paleoceanographic parameters, global distributions of these carbonate factories can be predicted using paleoclimate models. Figure 4 shows such an attempt to identify the oceanic regions that are the most favorable to the biochemical factory based on a single binary mask on simulated SST maxima (green shading). Interestingly, this simple approach captures well the spatial occurrences of this biochemical factory at a global scale (Fig. 4).

The Lower Aptian application of the carbonate factory concept confirms that specific carbonate platforms are related to specific paleoceanographic and paleoclimatic conditions (Fig. 5b). Shelf water bodies with high surface:volume ratios, i.e., homoclinal ramp system showing extensive platform extent and shallow water depths, within the arid tropical zone are subjected to strong heating and evaporation. Such a marine setting shows a specific carbonate production and associated evaporitic deposits, here referred to as biochemical factory, e.g., Gulf of Mexico. These areas are predictable at a global scale using paleoclimate models (Parrish et al. 1982). Away from these warmest zones, skeletal and reefal tropical platforms, here referred to as photozoan factory, develop in well-saturated, warm waters. No subtropical to warm-temperate carbonates were

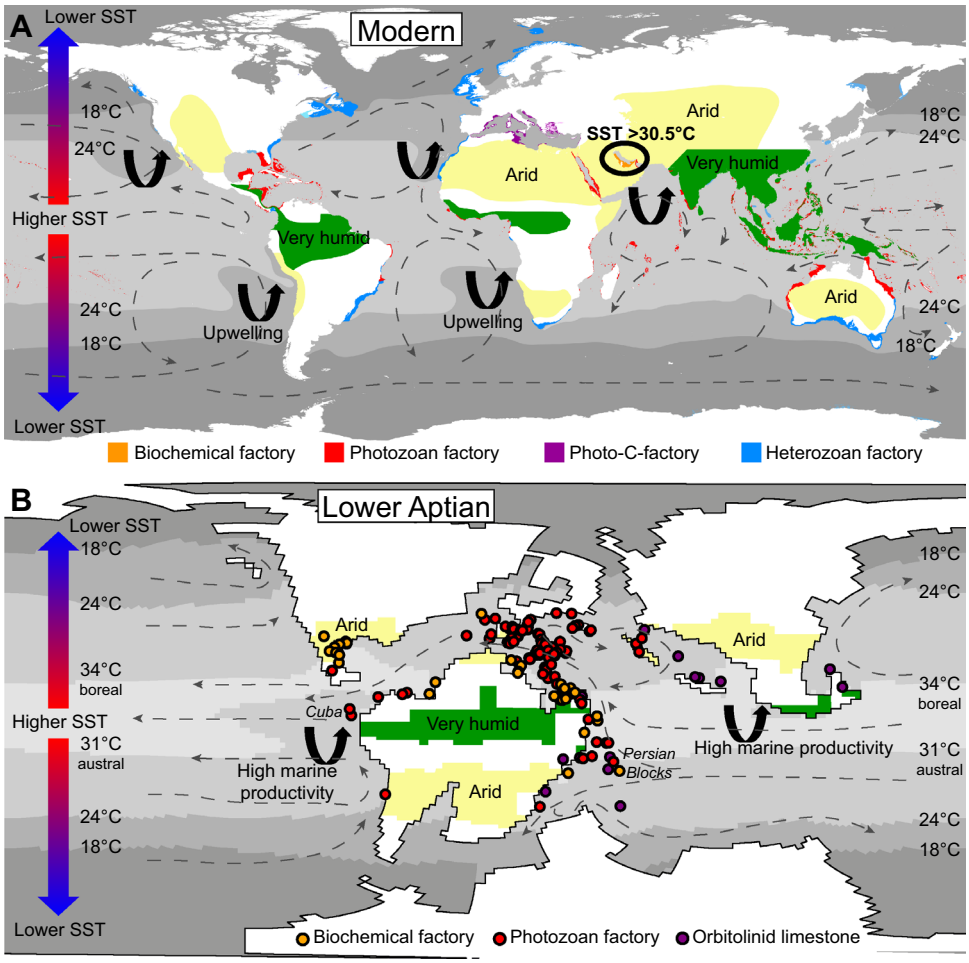

Fig. 5 Global climatic zones and carbonate factories in the **a** Modern and **b** Lower Aptian (120 Ma). Carbonate factory areas (**a**) and dots (**b**) correspond to bibliographic reference points of marine carbonate platforms. Background oceanic shading is the summer sea-surface temperature (SST) shown for each hemisphere. Summer SST corresponds to **a** the GLODAPv2 dataset (Lauvset et al. 2016; Olsen et al. 2016) and **b** climatic fields simulated using MITgcm ocean–atmosphere general circulation model shown at the climate model resolution (see "Methods" section for details). Continental masses are shaded white. Background continental shading represents the arid (yellow) and very humid (green) climatic zones; the Aptian equivalent of the modern equatorial and monsoonal climatic zone corresponds to the tropical rainforest and monsoon regime following the Köppen classification (cf. Peel et al. 2007). Aptian climatic fields were simulated using the FOAM model (Jacob 1997), because its atmospheric component is more sophisticated than the MITgcm model, thus providing more robust fields of surface temperature and precipitation

identified during this greenhouse period. Apart from bioclastic beds, i.e., Orbitolinids and molluscs others than rudists, i.e., heterozoan factory, which are often found within siliciclastic and volcaniclastic successions, e.g., eastern Asia, no other significant shallow-water carbonate deposits were identified.

The same pattern is observed in the Modern considering two different basinal settings, oceanographic conditions and carbonate factories within the same climatic zone. The hot and salty ramp of the Persian/Arabian Gulf hosts a unique modern biochemical factory in a foreland basin showing < 200 m maximum and 25 m mean water depths (Purser 1973; Anderson and Dyrssen 1994; Riegl et al. 2010; Riegl and Purkis 2012). Under similar climatic conditions, the Red Sea shows narrow shelves and a deeper basinal context in a rift-related basin showing > 2000 m maximum and 490 m mean water depths (Anderson and Dyrssen 1994; Omer 2010). The carbonate factory of the Red Sea is characterized by coral reefs and rimmed platform margins and is classified as photozoan (Purkis et al. 2012). Thus, on one hand, the carbonate production of the photozoan factory occurs in clear, warm waters, because photosynthetic processes are primarily controlled by light energy (Wilson 1975; James 1997; Schlager 2005; Hallock 2015; also cf. Pomar and Hallock 2008). On the other hand, the biochemical factory is found under the warmest and saltiest oceanic conditions, because carbonate precipitation of non-skeletal grains and microbes is primarily driven by biogeochemical processes (cf. Lees

1975; Dupraz et al. 2009; Schlager 2005; Bouton et al. 2016; Diaz and Eberli 2019; Fig. 5a). Environmental conditions of the biochemical factory, thus, relate to a restricted platform and basinal context that shows high surface:volume ratio. This simple, global-scale scheme might be related with (a) saturation that increases with increasing temperatures and salinity and (b) alkalinity that increases with salinity (Wilson 1975; Opdyke and Wilkinson 1990; Kleypas et al. 1999; Carter et al. 2014; Jiang et al. 2014; also cf. the "kettle effect" of Skelton and Gili 2012). Oceanographic conditions then derive from the direct relationship between climate and platform and basinal topography, which is controlled by geodynamics (Fig. 5).

Environmental affinities that are defined based on modern representatives of the biochemical factory seem to equally characterize their deep-time counter-parts such as the Aptian Gulf of Mexico (also cf. "Biochemical factory" section. Examples of the biochemical factory). It can, thus, be argued that the global-scale paleo-distributions of the biochemical factory are predictable using paleoclimate models (cf. Parrish et al. 1982). A priori, paleoenvironments of the biochemical factory are expected to occur on extensive ramps like epeiric seas and convergent tectonic settings such as foreland basins (cf. Burchette and Wright 1992) under arid tropical conditions. The Zagros Foreland Basin, e.g., Oligo-Miocene Asmari Formation (Van Buchem et al. 2010) and North American craton, e.g., Albian central Texas and Mississippian Central Montana high (Wilson 1975) represent potential examples of such a platform paleoenvironment. By contrast, shallow-water carbonates show different facies and architectures under humid equatorial conditions at least during the Cenozoic (Wilson 2012). These humid equatorial settings show warm temperatures, together with common clastic, fresh water, and nutrient influx. In terms of grain association and sedimentary profiles, specific features of equatorial carbonates compared to more classical tropical carbonates include common occurrence of heterotrophs and calcitic dominant mineralogies, common association with clastics and lack of coated grains or aggregates and evaporites (Wilson 2012). Beyond these differences, the photozoan factory is the best model to characterize most of these equatorial carbonate facies and stratigraphic architectures as shown by the presence of many examples of thick, aggrading offshore buildups under these paleoclimatic conditions, e.g., Luconia (Wilson 2002).

In summary, it is possible to define global-scale climatic zones of shallow-water marine carbonates based on SST, SSS, the marine primary productivity, and the basin geometry (Fig. 5). The photozoan factory is found within equatorial and tropical latitudes, i.e., warm temperatures, on the eastern side of continents, i.e., low marine productivities, preferentially in detached platform settings, i.e., away from terrigenous input and under well-agitated oceanic conditions. The biochemical factory occurs in arid tropical regions, i.e., the warmest temperatures, within relatively oceanographically restricted platforms, i.e., water bodies showing high surface:volume ratios such as homoclinal ramps, high salinities, and moderate hydrodynamics. The photo-C-factory, if present at all that is not the case during the Lower Aptian, is found in the subtropical and warm-temperate province (cf. Bensing et al. 2008; Michel et al. 2018). The heterozoan factory is found in upwelling regions, high latitudes, and terrigenous-influenced settings that are characterized by high marine primary productivity levels.

Limitation of the approach

A deterministic approach is interpretative

A major challenge in classifying carbonate sedimentary records into carbonate factories is the geological uncertainty associated with both the very limited record availability, i.e., limited sampling of a limited available rock record of a limited preserved sedimentary record, and the interpretative dimension of paleoenvironmental reconstructions that are themselves based on these limited data. Consequently, the classifications of grain associations (see Kindler and Wilson 2010), platform profiles, i.e., ramp versus shelf (e.g., Lessini Shelf, NE Italy; Frost 1981; Pomar et al. 2017) and architectures, e.g., cool-water ramp versus lowstand wedge (Marion Plateau, NE Australia; Hallock et al. 2006; Eberli et al. 2010) necessarily remain open to discussion. However, global trends show that the deterministic approach of the carbonate factory scheme is robust and that it permits the first-order prediction of global shallow-water carbonate occurrences based on paleoenvironmental constraints provided by paleoclimate models (Pohl et al. 2019; see Fig. 4; also cf. Schlager, 2005).

Evolution and the need of carbonate factory calibration

The relationship between a carbonate factory and paleoceanographic parameters is based on ecological principles and environmental parameter ranges which allow for a biota to thrive. The main ecological and physico-chemical principles remain valid through time. However, biota and paleoclimatic conditions were different in the past, e.g., atmospheric CO_2 concentrations and Mg:Ca ratio (Stanley and Hardie 1998; Hallock 2015). The ranges of parameter values such as SST, SSS, and marine productivities that were optimum for specific biota development varied through time (cf. extinct rudists in Pohl et al. 2019). Consequently, carbonate factories and especially grain associations have to be defined for each period of time (cf. James 1983; Kiessling et al. 2003). Then,

calibration of parameter value ranges for each carbonate factory is required and must be conducted using numerical modelling and based on reference points that are extracted from literature reviews (cf. Pohl et al. 2019).

Conclusions

We set the principles of a method that aims to consolidate the basics for spatial marine carbonate prediction at a global-scale following up on the carbonate factory approach. The conceptual scheme tends to integrate knowledge, methods, and classifications that are commonly used for relating carbonate sedimentation and paleoceanographic parameters. The method has proven to provide interesting insights into the distribution of Lower Aptian and Modern carbonate platforms. The conceptual scheme that is tested and validated by numerical modelling needs refinements and improvements, in particular considering that the carbonate factories and paleoceanographic parameter ranges have to be defined for each time period because of biota evolution and paleoclimatic changes.

The model seeks for consistent principles at a global scale relating paleoceanographic parameters, i.e., environment, climate and chemistry, and carbonate production, i.e., food web, metabolic and chemical energy for grains, and biota to develop and thrive. The model is first based on carbonate saturation and the (in)dependence upon this carbonate saturation by different carbonate factories. Carbonate saturation is estimated from SST and SSS. Carbonate factories appear to thrive for specific ranges along the environmental gradient of carbonate saturation. Marine primary productivity represents an additional oceanographic constraint on the global distributions of carbonate platforms. This conceptual scheme appears to be able to provide a simple, universal model of paleoclimatic zones of shallow-water marine carbonates.

Tectonic processes often stand as a local controlling factor that cannot be predicted at a global scale, e.g., initial topography, and creates large heterogeneities in sedimentary profiles and stratigraphic architectures. An exception of this pattern is the biochemical factory for which tectonic processes, e.g., convergence zones, define the sedimentary profile, e.g., homoclinal ramp of a foreland basin, and associated paleoceanographic conditions, i.e., carbonate production under relatively restricted paleoceanographic conditions.

Further studies are needed to go beyond the simple observations and understand the physico-chemico-ecological processes that are involved in carbonate precipitation modes. For instance, the role of alkalinity, which is related to increased salinities, in controlling carbonate precipitation modes at a basinal scale remains poorly constrained for different temperature-related carbonate saturation ranges, e.g., equatorial versus tropical versus warm-temperate regions.

Acknowledgements Thanks are expressed to Total E&P for funding a significant part of the project and for granting permission to publish. Patrick Sorriaux, Emmanuelle Poli (Total RD Carbonate), Jérôme Hennuy and Jeroen Kenter (Total ISS Carbonate-PIT Geology) are thanked for their interaction with the project, as well as several scientists from Aix-Marseille University-CEREGE including Alexandre Lettéron, RD and ISS Carbonate including Sara Drachenberg (Total, Pau) and Denis Allemand (Scientific Center of Monaco, CSM) for interesting discussions. The authors thank the 'SIGEO' GIS service at CEREGE for providing access to the ArcGIS software, the CEA/CCRT for providing access to the HPC resources of TGCC under the allocation 2014-012212 made by GENCI, Pierre Sepulchre (LSCE, Gif-sur-Yvette, France) for providing the Köppen code used for analysis of the FOAM output, and Christopher R. Scotese (Northwestern University, Evanston, IL, USA) for providing the Aptian paleogeographical reconstruction. We are grateful to Pamela Hallock and John J. G. Reijmer for their constructive reviews.

References

Anderson L, Dyrssen D (1994) Alkalinity and total carbonate in the Arabian Sea. Carbonate depletion in the Red Sea and Persian Gulf. Mar Chem 47:195–202

Arp G, Reimer A, Reitner J (1999) Calcification in cyanobacterial biofilms of alkaline salt lakes. Eur J Sediment Res 73:105–127

Arp G, Reimer A, Reitner J (2003) Microbialite formation in seawater of increased alkalinity, Satonda Crater Lake, Indonesia. Eur J Phycol 34:393–403

Bassi D, Nebelsick JH (2010) Components, facies and ramps: redefining Upper Oligocene shallow water carbonates using coralline red algae and larger foraminifera (Venetian area, northeast Italy). Palaeogeogr Palaeoclimatol Palaeoecol 295:258–280

Beckwith ST, Byrne RH, Hallock P (2019) Riverine calcium endmembers improve coastal saturation state calculations and reveal regionally variable calcification potential. Front Mar Sci 6:169. https://doi.org/10.3389/fmars.2019.00169

Bedout DG, Budd DA, Schatzinger RA (1981) Depositional and diagenetic history of the Sligo and Hosston Formations (Lower Cretaceous) in South Texas. The University of Texas at Austin, Bureau of Economic Geology, Report of Investigations No. 109

Bensing JP, James NP, Beauchamp B (2008) Carbonate deposition during a time of mid-latitude ocean cooling: early Permian subtropical sedimentation in the Sverdrup Basin, Arctic Canada. J Sediment Res 78:2–15

Betzler C, Brachert TC, Nebelsick J (1997) The warm temperate carbonate province–A review of facies, zonations, and delimitations. Courier Forschungs-Institut Senckenberg 201:83–99

Birkeland C (1987) Nutrient availability as a major determinant of differences among coastal hard-substratum communities in different regions of the tropics. In: Birkeland C (ed) Differences between Atlantic and Pacific tropical marine coastal systems: community structure, ecological processes, and productivity. UNESCO, Paris, pp 45–90

Bosellini A, Russo A, Schroeder R (1999) Stratigraphic evidence for an early Aptian sea-level fluctuation: the Graua limestone of southeastern Ethiopia. Cretac Res 20:783–791

Bosence DWJ (1983) Coralline algal reef frameworks. J Geol Soc Lond 140:365–376

Bosence DWJ, Pedley HM (1982) Sedimentology and palaeoecology of a Miocene coralline algal biostrome from the Maltese Islands. Palaeogeogr Palaeoclimatol Palaeoecol 38:9–43

Bouton A, Vennin E, Pace A, Bourillot R, Dupraz C, Thomazo C, Brayard A, Désaubliaux G, Visscher PT (2016) External controls on the distribution, fabrics and mineralization of modern microbial mats in a coastal hypersaline lagoon, Cayo Coco (Cuba). Sedimentology 63:972–1016

Bover-Arnal T, Ferrandez-Cañadell C, Aguirre J, Esteban M, Fernández-Carmona J, Albert-Villanueva E, Salas R (2017) Late Chattian platform carbonates with benthic foraminifera and coralline algae from the SE Iberian Plate. Palaios 32:61–82

Brachert TC, Forst MH, Pais JJ, Legoinha P, Reijmer JJG (2003) Lowstand carbonates, highstand sandstones? Sedimtary Geol 155:1–12

Brewer PG, Dyrssen D (1985) Chemical oceanography of the Persian Gulf. Prog Oceanogr 14:41–55

Burchette TP, Wright VP (1992) Carbonate ramp depositional systems. Sedimtary Geol 79:3–57

Busson G, Albanesi C (1967) Le Crétacé inférieur et le Jurassique terminal de l'Extrême-sud tunisien. Rivista Italiana de Paleontologia 73:591–634

Busson G, Dufaure P, Foury G (1966) Nouvelles observations sur l'âge de la transgression crétacée au Tebaga de Médenine et au Sahara tunisien. Compte Rendu sommaire de la Société Géologique de France 3:135–136

Camoin GF, Cabioch G, Eisenhauer A, Braga JC, Hamelin B, Lericolais G (2006) Environmental signifi cance of microbialites in reef environments during the last deglaciation. Sedimtary Geol 185:277–295

Campbell RJ, Haig DW (1999) Bathymetric changes during early Cretaceous intracratonic marine transgression across the northeastern Eromanga Basin, Australia. Cretac Res 20:403–446

Carannante G, Esteban M, Milliman JD, Simone L (1988) Carbonate lithofacies as paleolatitude indicators: problems and limitations. Sediment Geol 60:333–346

Carter BR, Toggweiler JR, Key RM, Sarmiento JL (2014) Processes determining the marine alkalinity and calcium carbonate saturation state distributions. Biogeosciences 11:1–14

Case DH, Pasulka AL, Marlow JJ, Grupe BM, Levin LA, Orphan VJ (2015) Methane seep carbonates host distinct, diverse, and dynamic microbial assemblages. MBio. https://doi.org/10.1128/mBio.01348-15

Chazottes V, Reijmer JJG, Cordier E (2008) Sediment characteristics in reef areas influenced by eutrophication-related alterations of benthic communities and bioerosion processes. Mar Geol 250:114–127

Couce E, Ridgwell AJ, Hendy EJ (2012) Environmental controls on the global distribution of shallow-water coral reefs. J Biogeogr 39:1508–1523

Diaz MR, Eberli GP (2019) Decoding the mechanism of formation in marine ooids: a review. Earth Sci Rev. https://doi.org/10.1016/j.earscirev.2018.12.016

Diaz RJ, Rosenberg R (1995) Marine benthic hypoxia: a review of its ecological effects and the behavioural responses of benthic macrofauna. Oceanogr Mar Biol Annu Rev 33:245–303

Dupraz C, Reid RP, Braissant O, Decho AW, Norman RS, Visscher PT (2009) Processes of carbonate precipitation in modern microbial mats. Earth Sci Rev 96:141–162

Dutertre M, Grall J, Ehrhold A, Hamon D (2015) Environmental factors affecting maerl bed structure in Brittany (France). Eur J Phycol 50:371–383

Eberli GP, Anselmetti FS, Isern AR, Delius H (2010) Timing of changes in sea-level and currents along Miocene platforms on the Marion Plateau, Australia. In: Morgan WA, George AD, Harris PM, Kupecz JA, Sarg JF (eds) Cenozoic carbonate systems of Australasia, vol 95. SEPM Society for Sedimentary Geology, Tulsa, pp 219–242

Embry JC, Vennin E, van Buchem FSP, Schroeder R, Pierre C, Aurell M (2010) Sequence stratigraphy and carbon isotope stratigraphy of an Aptian mixed carbonate-siliciclastic platform to basin transition (Galve sub-basin, NE Spain). In: van Buchem FSP, Gereds KD, Esteban M (eds) Mesozoic and cenozoic carbonate systems of the Mediterranean and the Middle East: stratigraphic and diagenetic reference models, vol 329. Geological Society of London, London, pp 113–143

Föllmi KB, Bodin S, Bodin S, Linder P (2006) Interactions between environmental change and shallow water carbonate buildup along the northern Tethyan margin and their impact on the Early Cretaceous carbon isotope record. Paleoceanography 21(4):PA4211. https://doi.org/10.1029/2006PA001313

Föllmi KB, Bodin S, Bodin S, Linder P, van de Schootbrugge B (2007) Unlocking paleo-environmental information from early Cretaceous shelf sediments in the Helvetic Alps: stratigraphy is the key! Swiss J Geosci 100:349–369

Frank TD, Pritchard JM, Fielding CR, Mory AJ (2012) Cold-water carbonate deposition in a high-latitude, glacially influenced permian seaway (southern carnarvon basin, Western Australia). Aust J Earth Sci 59:479–494

Franseen EK (2006) Mississippian (Osagean) shallow-water, mid-latitude siliceous sponge spicule and heterozoan carbonate facies: an example from Kansas with implications for Regional controls and distribution of potential reservoir facies. Current Research in Earth Sciences: Kansas Geological Survey Bulletin 252, part 1. http://www.kgs.ku.edu/Current/2006/franseen/index.html. Accessed 17 May 2019

Freiwald A (1998) Modern nearshore cold-temperate calcareous sediments in the Troms District, northern Norway. J Sediment Res 68:763–776

Freiwald A, Fosså JH, Grehan A, Koslow T, Roberts JM (2004) Cold-water coral reefs. UNEP-WCMC, Cambridge

Fritz DA, Belsher TW, Medlin JM, Stubbs JL, Wright RP, Harris PM (2000) New exploration concepts for the Edwards and Sligo margins, cretaceous of onshore Texas. AAPG Bull 84:905–922

Frost SH (1981) Oligocene reef coral biofacies of the Vicentin, northern Italy. In: Toomey DF (ed) European fossil reef models, vol 30. SEPM Society for Sedimentary Geology, Tulsa, pp 483–539

Gattuso J, Frankignoulle M, Bourge I, Romaine S, Buddemeier RW (1998) Effect of calcium carbonate saturation of seawater on coral calcification. Glob Planet Change 18:37–46

Gili E, Negra M, Skelton PW (2003) North African Cretaceous carbonate platform systems, vol 28. NATO science series IV, earth and environmental sciences. Springer, New York

Halfar J, Godinez-Orta L, Mutti M, Valdez-Holguin JE, Borges JM (2004) Nutrient and temperature controls on modern carbonate production: an example from the Gulf of California, Mexico. Geology 32:213–216

Halfar J, Godinez-Orta L, Mutti M, Valdez-Holguin JE, Borges JM (2006) Carbonates calibrated against oceanographic parameters along a latitudinal transect in the Gulf of California, Mexico. Sedimentology 53:297–320

Hallock P (2001) Coral reefs, carbonate sediments, nutrients, and global change. In: Stanley GD (ed) The history and sedimentology of ancient reef systems. Kluwer, New York, pp 387–427

Hallock P (2015) Changing influences between life and limestones in earth history. In: Birkeland C (ed) Coral reefs in the Anthropocene. Springer, Dordrecht, pp 17–42

Hallock P, Schlager W (1986) Nutrient excess and the demise of coral reefs and carbonate platforms. Palaios 1:389–398

Hallock P, Sheps K, Chapronière G, Howell M (2006) Larger benthic foraminifers of the Marion Plateau, northeastern Australia (ODP Leg 194): comparison of faunas from bryozoan (sites 1193

and 1194) and red algal (sites 1196–1198) dominated carbonate platforms. In: Anselmetti FS, Isern AR, Blum P, Betzler C (eds) Proceedings of the Ocean Drilling Program, scientific results, vol 194, issue 2, pp 1–31

Henrich R, Freiwald A, Betzler C, Bader B, Schäfer P, Samtleben C, Brachert TTC, Wehrmann A, Zankl H, Kühlmann DHH (1995) Controls on modern carbonate sedimentation on warm-temperate to Arctic coasts, shelves and seamounts in the Northern Hemisphere: implications for fossil counterparts. Facies 32:71–108

Henrich R, Freiwald A, Birkett T, Schäfer P (1997) Evolution of an Arctic open-shelf carbonate platform, Spitsbergen Bank (Barents Sea). In: James NP, Clarke JAD (eds) Cool-water carbonates, vol 56. SEPM Society for Sedimentary Geology, Tulsa, pp 163–181

Iba Y, Sano SI, Miura T (2011) Orbitolinid foraminifers in the Northwestern Pacific: their taxonomy and stratigraphy. Micropaleontology 57:163–171

Jacob RL (1997) Low frequency variability in a simulated atmosphere ocean system. PhD thesis, University of Wisconsin-Madison

James NP (1983) Reef environment. In: Scholle PA, Bebout DG, Moore CH (eds) Carbonate depositional environments. American Association of Petroleum Geologists, Tulsa, pp 346–440

James NP (1997) The cool-water carbonate depositional realm. In: James NP, Clarke J (eds) Cool-water carbonates, vol 56. SEPM Society for Sedimentary Geology, Tulsa, pp 1–20

James NP, Bone Y (2011) Neritic carbonate sediments in a temperate realm—South Australia. Springer, Dordrecht

James NP, Bourque PA (1992) Reefs and mounds. In: Walker RG, James NP (eds) Facies models, response to sea level change, vol 1. Geological Association of Canada, St. John's, pp 323–347

James NP, Jones BG (2015) Origin of carbonate rocks. Wiley, Hoboken

James NP, Lukasik JJ (2010) Cool- and cold-water carbonates. In: James NP, Dalrymple RW (eds) Facies models 4. Geological Association of Canada, St. John's, pp 371–399

James NP, Collins LB, Bone Y, Hallock P (1999) Subtropical carbonates in a temperate realm: modern sediments on the southwest Australian shelf. J Sediment Res 69:1297–1321

James NP, Bone Y, Brown KM, Cheshire A (2009a) Calcareous epiphyte production in cool-water carbonate seagrass depositional environments; Southern Australia. In: Swart PK, Eberli GP, McKenzie JA (eds) Perspectives in carbonate geology: a tribute to the career of Robert Nathan Ginsburg, vol 41. Wiley, Hoboken, pp 123–148

James NP, Frank TD, Fielding CR (2009b) Carbonate sedimentation in a permian high-latitude, subpolar depositional realm: Queensland, Australia. J Sediment Res 79:125–143

James NP, Reid CM, Bone Y, Levings A, Malcolm I (2013) The macroalgal carbonate factory at a cool-to-warm temperate marine transition, Southern Australia. Sediment Geol 291:1–26

Jiang ZP, Tyrrell T, Hydes DJ, Dai M, Hartman SE (2014) Variability of alkalinity and the alkalinity-salinity relationship in the tropical and subtropical surface ocean. Glob Biogeochem Cycl. https://doi.org/10.1002/2013gb004678

Jiang LQ, Feely RA, Carter BR, Greeley DJ, Gledhill DK, Arzayus KM (2015) Climatological distribution of aragonite saturation state in the global oceans. Glob Biogeochem Cycl 29:1656–1673. https://doi.org/10.1002/2015gb005198

Jones NS, Ridgwell AJ, Hendy EJ (2015) Evaluation of coral reef carbonate production models at a global scale. Biogeosciences 12:1339–1356

Kiessling W, Flügel E, Golonka J (1999) Paleoreef Maps: evaluation of a comprehensive database on Phanerozoic reefs. AAPG Bull 83:1552–1587

Kiessling W, Flügel E, Golonka J (2003) Patterns of Phanerozoic carbonate platform sedimentation. Lethaia 36:195–226

Kindler P, Wilson MEJ (2010) Carbonate grain associations: their use and environmental significance, a brief review. In: Mutti M, Piller WE, Betzler C (eds) Carbonate systems during the Oligocene–Miocene climatic transition, vol 42. Blackwell, Oxford, pp 35–48

Kleypas J (2015) Invisible barriers to dispersal. Science 348:1086–1087

Kleypas JA, McManus JW, Menez LAB (1999) Environmental limits to coral reef development: where do we draw the line? Am Zool 39:146–159

Klicpera A, Michel J, Westphal H (2015) Facies patterns of a tropical heterozoan carbonate platform under eutrophic conditions: the Banc d'Arguin, Mauritania. Facies 61:421. https://doi.org/10.1007/s10347-014-0421-5

Lauvset SK, Key RM, Olsen A, van Heuven S, Velo A, Lin X, Schirnick C, Kozyr A, Tanhua T, Hoppema M, Jutterström S, Steinfeldt R, Jeansson E, Ishii M, Perez FF, Suzuki T, Watelet S (2016) A new global interior ocean mapped climatology: the GLODAP version 2. Earth Syst Sci Data 8:325–340. https://doi.org/10.5194/essd-8-325-2016

Lees A (1975) Possible influence of salinity and temperature on modern shelf carbonate sedimentation. Mar Geol 19:159–198

Lees A, Buller AT (1972) Modern temperate water and warm water shelf carbonate sediments contrasted. Mar Geol 13:M67–M73

Lehmann C, Osleger DA, Montañez IP, Sliter W, Arnaud-Vanneau A, Banner J (1999) Evolution of Cupido and Coahuila carbonate platforms, Early Cretaceous, northeastern Mexico. GSA Bull 111:1010–1029

Lokier SW, Wilson MEJ, Burton LM (2009) Marine biota response to clastic sediment influx: a quantitative approach. Palaeogeogr Palaeoclimatol Palaeoecol 281:25–42

Lowery JG, Rankey EC (2017) Nearshore influences of upwelling, waves, and currents on a tropical carbonate ramp: holocene, northwestern Yucatan shelf, Mexico. J Sediment Res 87:546–566

Lunt DJ, Farnsworth A, Loptson C, Foster GL, Markwick P et al (2016) Palaeogeographic controls on climate and proxy interpretation. Clim Past 12:1181–1198. https://doi.org/10.5194/cp-12-1181-2016-supplement

Markello JR, Koepnick RB, Waite LE, Collins JF (2008) The carbonate analogs through time (CATT) hypothesis and the global atlas of carbonate fields—a systematic and predictive look at Phanerozoic carbonate systems. In: Lukasik J, Schlager W (eds) Controls on carbonate platform and reef development, vol 89. SEPM Society for Sedimentary Geology, Tulsa, pp 15–46

Martin CS, Giannoulaki M, De Leo F et al (2014) Coralligenous and maërl habitats: predictive modelling to identify their spatial distributions across the Mediterranean Sea. Nat Sci Rep 4:5073. https://doi.org/10.1038/srep05073

Martindale W, Boreen TD (1997) Temperature-stratified Mississippian carbonates as hydrocarbon reservoirs—examples from the Foothills of the Canadian Rockies. In: James NP, Clarke JAD (eds) Cool-water carbonates, vol 56. SEPM Society for Sedimentary Geology, Tulsa, pp 391–409

Martindale RC, Corsetti FA, James NP, Bottjer DJ (2015) Paleogeographic trends in Late Triassic reef ecology from northeastern Panthalassa. Earth Sci Rev 142:18–37

Messabeb H, Contamine F, Cézac P, Serin JP, Gaucher EC (2016) Experimental measurement of CO_2 solubility in aqueous NaCl solution at temperature from 323.15 to 423.15 K and pressure of up to 20 Mpa. J Chem Eng Data 61:3573–3584

Michel J, Mateu-Vicens G, Westphal H (2011a) Modern heterozoan carbonates from a eutrophic tropical shelf (Mauritania). J Sediment Res 81:641–655

Michel J, Westphal H, von Cosel R (2011b) The mollusk fauna of soft sediments from the tropical, upwelling-influenced shelf of Mauritania (northwestern Africa). Palaios 26:447–460

Michel J, Borgomano J, Reijmer JJG (2018) Heterozoan carbonates: when, where and why? A synthesis on parameters controlling carbonate production and occurrences. Earth Sci Rev 182:50–67

Muir PR, Wallace CC, Done T, Aguirre JD (2015) Limited scope for latitudinal extension of reef corals. Science 348:1135–1138
Nelson CS (1988) An introductory perspective on non-tropical shelf carbonates. Sediment Geol 60:3–12
Nelson CS, James NP (2000) Marine cements in mid-Tertiary cool-water limestones of New Zealand and southern Australia. Sedimentology 47:609–629
Nelson CS, Keane SL, Head PS (1988) Non-tropical carbonate deposits on the modern New Zealand shelf. Sed Geol 60:71–94
Nelson CS, Winefield PR, Hood SD, Caron V, Pallentin A, Kamp PJJ (2003) Pliocene Te Aute limestones, New Zealand: expanding concepts for cool-water shelf carbonates. N Z J Geol Geophys 46:407–424
Nilsson HC, Rosenberg R (2000) Succession in marine benthic habitats and fauna in response to oxygen deficiency: analysed by sediment profile-imaging and by grab samples. Mar Ecol Prog Ser 197:139–149
O'Connell LG, James NP, Doubell M, John F (2016) Oceanographic controls on shallow-water temperate carbonate sedimentation: Spencer Gulf, South Australia. Sedimentology 63:105–135
O'Brien CL, Robinson SA, Pancost RD, Damsté JSS, Schouten S, Lunt DJ et al (2017) Cretaceous sea-surface temperature evolution: constraints from TEX86 and planktonic foraminiferal oxygen isotopes. Earth Sci Rev 172:224–247
Olsen A, Key RM, van Heuven S, Lauvset SK, Velo A, Lin X, Schirnick C, Kozyr A, Tanhua T, Hoppema M, Jutterström S, Steinfeldt R, Jeansson E, Ishii M, Pérez FF, Suzuki T (2016) The Global Ocean Data Analysis Project version 2 (GLODAPv2)—an internally consistent data product for the world ocean. Earth Syst Sci Data 8:297–323. https://doi.org/10.5194/essd-8-297-2016
Omer WMM (2010) Ocean acidification in the Arabian Sea and the Red Sea. Dissertation, Undergraduate Honors Theses, University of Bergen. http://bora.uib.no/bitstream/handle/1956/7538/71959070.pdf?sequence=1. Accessed 22 Jan 2019
Opdyke BN, Wilkinson BH (1990) Paleolatitude distribution of Phanerozoic marine ooids and cements. Palaeogeogr Palaeoclimatol Palaeoecol 78:135–148
Opdyke BN, Wilkinson BH (1993) Carbonate mineral saturation state and cratonic limestone accumulation. Am J Sci 293:217–234
Pace A, Bourillot R, Bouton A, Vennin E, Galaup S, Bundeleva I, Patrier P, Dupraz C et al (2016) Microbial and diagenetic steps leading to the mineralisation of Great Salt Lake microbialites. Sci Rep 6:31495. https://doi.org/10.1038/srep31495
Parrish JT (1982) Upwelling and petroleum source beds, with reference to paleozoic. AAPG Bull 66:750–774
Parrish JT (1995) Paleogeography of Corg-rich rocks and the preservation versus production controversy. In: Huc AY (ed) Paleogeography, paleoclimate, and source rocks AAPG studies in geology, vol 40. American Association of Petroleum Geologists, Tulsa, pp 1–20
Parrish JT, Curtis RL (1982) Atmospheric circulation, upwelling, and organic-rich rocks in the Mesozoic and Cenozoic eras. Palaeogeogr Palaeoclimatol Palaeoecol 40:31–66
Parrish JT, Scotese CR, Ziegler AM (1982) Rainfall patterns and the distribution of coals and evaporites in the Mesozoic and Cenozoic. Palaeogeogr Palaeoclimatol Palaeoecol 40:67–101
Pedley HM, Carannante G (2006) Cool-water carbonate ramps: a review. In: Pedley HM, Carannante G (eds) Cool-water carbonates: depositional systems and palaeoenvironmental controls, vol 255. Geological Society of London, London, pp 1–9
Peel MC, Finlayson BL, Mcmahon TA (2007) Updated world map of the Köppen–Geiger climate classification. EGU Hydrol Earth Syst Sci Discuss 11:1633–1644
Pérès JM, Picard J (1964) Nouveau manuel de bionomie benthique de la Mer Méditerranée. Recueil de la Station Marine d'Endoume 31, pp 1–137. http://paleopolis.rediris.es/BrachNet/REF/Download/Manuel.html. Accessed 12 June 2016
Perry CT, Beavington-Penney SJ (2005) Epiphytic calcium carbonate production and facies development within sub-tropical seagrass beds, Inhaca Island, Mozambique. Sediment Geol 174:161–176
Perry CT, Hepburn LJ (2008) Syn-depositional alteration of coral reef framework through bioerosion, encrustation and cementation: taphonomic signatures of reef accretion and reef depositional events. Earth Sci Rev 86:106–144
Pittet B, van Buchem FSP, Hillgärtner H, Razin P, Grötsch J, Droste H (2002) Ecological succession, palaeoenvironmental change, and depositional sequences of Barremian-Aptian shallow-water carbonates in northern Oman. Sedimentology 49:555–581
Pohl A, Laugié M, Borgomano J, Michel J, Lanteaume C, Scotese CR, Frau C, Poli E, Masse JP, Donnadieu Y (2019) Quantifying the paleogeographical driver of Cretaceous carbonate platforms development using paleoecological niche modeling. Palaeogeogr Palaeoclimatol Palaeoecol 514:222–232
Pomar L (2001) Types of carbonate platforms: a genetic approach. Basin Res 13:313–334
Pomar L, Hallock P (2008) Carbonate factories: a conundrum in sediment geology. Earth Sci Rev 87:134–169
Pomar L, Mateu-Vicens G, Morsilli M, Brandano M (2014) Carbonate ramp evolution during the late Oligocene (Chattian), Salento peninsula, southern Italy. Palaeogeogr Palaeoclimatol Palaeoecol 404:109–132
Pomar L, Baceta JI, Hallock P, Mateu-Vicens G, Basso D (2017) Reef building and carbonate production modes in the west-central Tethys during the Cenozoic. Mar Pet Geol 83:261–304. https://doi.org/10.1016/j.marpetgeo.2017.03.015
Prosorovsky VA (1990) The Urgonian facies of central Asia. Cretac Res 11:253–260
Purkis SJ, Harris PM, Ellis J (2012) Patterns of sedimentation in the contemporary Red Sea as an analog for ancient carbonates in rift settings. J Sediment Res 82:859–870
Purser BH (1973) The Persian Gulf. Holocene carbonate sedimentation and diagenesis in a shallow epicontinental sea. Springer, New York
R Core Team (2013) R: a language and environment for statistical computing. R Foundation for Statistical Computing, Vienna. http://www.R-project.org/
Rao CP (1996) Modern carbonates: tropical, temperate, polar—introduction to sedimentology and geochemistry. University of Tasmania, Hobbart
Reijmer JJG (2014) Carbonate Factories. In: Harff J, Meschede M, Petersen S, Thiede J (eds) Encyclopedia of marine geosciences. Springer, Dordrecht, pp 80–84. https://doi.org/10.1007/978-94-007-6644-0
Reijmer JJG, Bauch T, Schäfer P (2012) Carbonate facies patterns in surface sediments of upwelling and non-upwelling shelf environments (Panama, East Pacific). Sedimentology 59:32–56
Ridgwell AJ, Zeebe RE (2005) The role of the global carbonate cycle in the regulation and evolution of the Earth system. Earth Planet Sci Lett 234:299–315
Riding R, Liang L (2005a) Geobiology of microbial carbonates: metazoan and seawater saturation state influences on secular trends during the Phanerozoic. Palaeogeogr Palaeoclimatol Palaeoecol 219:101–115
Riding R, Liang L (2005b) Seawater chemistry control of marine limestone accumulation over the past 550 million years. Rev Esp Micropaleontol 37:1–11
Riding R, Liang L, Lee J-H, Virgone A (2019) Influence of dissolved oxygen on secular patterns of marine microbial carbonate abundance during the past 490 Myr. Palaeogeogr Palaeoclimatol Palaeoecol 514:135–143

Riegl BM, Purkis SJ (2012) Coral reefs of the Gulf: adaptation to climatic extremes. Springer, Dordrecht

Riegl B, Poiriez A, Janson X, Bergman KL (2010) The Gulf: Facies belts, physical, chemical, and biological parameters of sedimentation on a carbonate ramp. In: Westphal H, Riegl B, Eberli GP (eds) Carbonate depositional systems: Assessing dimensions and controlling parameters. The Bahamas, Belize and the Persian/Arabian Gulf. Springer, Dordrecht, pp 145–213

Riosmena-Rodríguez R, Nelson W, Aguirre J (2017) Rhodolith/Maërl beds: a global perspective. Coastal Research Library, vol 15. Springer, Cham

Saraswat R, Kouthanker M, Kurtarkar SR, Nigam R, Naqvi SWA, Linshy VN (2015) Effect of salinity induced pH/alkalinity changes on benthic foraminifera: a laboratory culture experiment. Estuar Coast Shelf Sci 153:96–107

Schlager W (2000) Sedimentation rates and growth potential of tropical, cool-water and mud-mound carbonate factories. In: Insalaco E, Skelton P, Palmer TJ (eds) Carbonate platform systems: components and interactions, vol 178. Geological Society of London, London, pp 217–227

Schlager W (2003) Benthic carbonate factories of the Phanerozoic. Int J Earth Sci 92:445–464

Schlager W (2005) Carbonate sedimentology and sequence stratigraphy. SEPM concepts in sedimentology and paleontology No. 8, Tulsa, Oklahoma

Schlagintweit F, Bucur II, Rashidi K, Saberzadeh B (2013) *Praeorbitolina claveli* n.sp. (benthic foraminifera) from the Lower Aptian sensu lato (Bedoulian) of Central Iran. Notebooks in Geology CG2013_L04:255–272

Scotese CR (2014a) Late Cretaceous Atlas of Paleogeograhic Maps, PALEOMAP Atlas for ArcGIS, volume 2, The Cretaceous, Maps 16–22, Mollweide project, PALEOMAP Project, Evanston, IL. https://doi.org/10.13140/2.1.4691.3284

Scotese CR (2014b) Early Cretaceous Atlas of Paleogeograhic Maps, PALEOMAP Atlas for ArcGIS, volume 2, The Cretaceous, Maps 23–31, Mollweide project, PALEOMAP Project, Evanston, IL. https://doi.org/10.13140/2.1.4099.4560

Scott RW (1993) Early Cretaceous carbonate platform, U.S. gulf Coast. In: Simo JA, Scott RW, Masse JP (eds) Cretaceous carbonate platforms, AAPG Memoir 56. American Association of Petroleum Geologists, Tulsa, pp 97–110

Simo JA, Scott RW, Masse JP (1993) Cretaceous carbonate platforms. AAPG Memoir 56. American Association of Petroleum Geologists, Tulsa

Skelton PW, Gili E (2012) Rudists and carbonate platforms in the Aptian: a case study on biotic interactions with ocean chemistry and climate. Sedimentology 59:81–117

Stanley MS, Hardie LA (1998) Secular oscillations in the carbonate mineralogy of reefbuilding and sediment-producing organisms driven by tectonically forced shifts in seawater chemistry. Palaeogeogr Palaeoclimatol Palaeoecol 144:3–19

Summerhayes CP, Milliman JD, Briggs SR, Bee AG, Hogan C (1976) Northwest African shelf sediments: influence of climate and sedimentary processes. J Geol 84:277–300

Takahashi M (1983) Space-time distribution of the Late Mesozoic to Early Cenozoic magmatism in East Asia and its tectonic implications. In: Hashimoto M, Uyeda S (eds) Accretion tectonics in the Circum-Pacific regions. Terrapub, Tokyo, pp 69–88

Tambutté S, Holcomb M, Ferrier-Pagès C, Reynaud S, Tambutté E, Zoccola D, Allemand D (2011) Coral biomineralization: from the gene to the environment. J Exp Mar Biol Ecol 408:58–78

Tomas S, Zitzmann M, Homann M, Rumpf M, Amour F, Benisek M, Marcano G, Mutti M, Betzler C (2010) From ramp to platform: building a 3D model of depositional geometries and facies architectures in transitional carbonates in the Miocene, northern Sardinia. Facies 56:195–210

Tomassetti L, Brandano M (2013) Sea level changes recorded in mixed siliciclastic–carbonate shallow-water deposits: the Cala di Labra Formation (Burdigalian, Corsica). Sediment Geol 294:58–67

Track PD (1936) Relation of salinity to the calcium carbonate content of marine sediments. US Geological Survey, Professional Paper 186-N, Washington, pp 273–299

Tucker ME, Wright VP (1990) Carbonate sedimentology. Blackwell, Oxford

van Buchem FSP, Allan TL, Laursen GV, Lotfpour M, Moallemi A, Monibi S, Motiei H, Pickard NAH, Tahmasbi AR, Vedrenne V, Vincent B (2010) Regional stratigraphic architecture and reservoir types of the Oligo-Miocene deposits in the Dezful Embayment (Asmari and Pabdeh Formations) SW Iran. Geol Soc Lond Spec Publ 329:219–263

Veron JEN (1995) Corals in space and time. Comstock/Cornell, Ithaca

Wasserman HN (2011) A global view of coral reef cementation as a function of seawater aragonite saturation states. Dissertation, Undergraduate Honors Theses 722, University of Colorado Boulder http://scholar.colorado.edu/honr_theses/722/. Accessed 09 Jan 2019

Wells SM (1988a) Coral reefs of the world. Volume 1: Atlantic and Eastern Pacific. UNEP Regional Seas Directories and Bibliographies, IUCN, Gland, Switzerland and Cambridge, UK/UNEP, Nairobi, Kenya. ISBN: 2-88032-943-4

Wells SM (1988b) Coral reefs of the world. Volume 2: Indian Ocean, Red Sea and Gulf. UNEP Regional Seas Directories and Bibliographies, IUCN, Gland, Switzerland and Cambridge, UK/UNEP, Nairobi, Kenya. ISBN: 2-88032-944-2

Wells SM (1988c) Coral reefs of the world. Volume 3: Central and Western Pacific. UNEP Regional Seas Directories and Bibliographies, IUCN, Gland, Switzerland and Cambridge, UK/UNEP, Nairobi, Kenya. ISBN: 2-88032-945-0

Westphal H, Halfar J, Freiwald A (2010a) Heterozoan carbonates in subtropical to tropical settings in the present and past. Int J Earth Sci 99:S153–S169

Westphal H, Riegl B, Eberli GP (2010b) Carbonate depositional systems: Assessing dimensions and controlling parameters—The Bahamas, Belize and the Persian/Arabian Gulf. Springer, Dordrecht

Whalen MT (1995) Barred basins: A model for eastern ocean basin carbonate platforms. Geology 23:625–628

Wilson JL (1975) Carbonate facies in geologic history. Springer, Berlin

Wilson MEJ (2002) Cenozoic carbonates in Southeast Asia: implications for equatorial carbonate development. Sediment Geol 147:295–428

Wilson MEJ (2008) Global and regional influences on equatorial shallow-marine carbonates during the Cenozoic. Palaeogeogr Palaeoclimatol Palaeoecol 265:262–274

Wilson MEJ (2012) Equatorial carbonates: an earth systems approach. Sedimentology 59:1–31

Wilson JL, Ward WC (1993) Early Cretaceous carbonate platforms of northeastern and east-central Mexico. In: Simo JA, Scott RW, Masse JP (eds) Cretaceous carbonate platforms, AAPG Memoir 56. American Association of Petroleum Geologists, Tulsa, pp 35–50

Wold S, Esbensen K, Geladi P (1987) Principal component analysis. Chemometr Intell Lab Syst 2:37–52

Wood R (1993) Nutrients, predation and the history of reef-building. Palaios 8:526–543

Yates KK, Robbins LL (2001) Microbial lime-mud production and its relation to climate change. In: Gerhard LC, Harrison WE, Hanson BM (eds) Geological perspectives of global climate change. AAPG Studies in Geology, vol 47. American Association of Petroleum Geologists, Tulsa, pp 267–283